Zeolitic and Layered Materials

Steven L. Suib

U-60, Departments of Chemistry and Chemical Engineering and Institute of Materials Science, University of Connecticut, Storrs, Connecticut 06269-3060

Received July 1, 1992 (Revised Manuscript Received October 29, 1992)

Contents

I.	Introduction	803
II.	Synthesis	803
	A. Three-Dimensional Materials	803
	1. New Materials	803
	2. Isomorphous Substitution	808
	B. Layered Materials	808
III.	Characterization	811
	A. Magnetic Methods	811
	1. Nuclear Magnetic Resonance	811
	2. Electron Paramagnetic Resonance	813
	B. Optical Methods	815
	1. Raman	815
	2. Luminescence	816
	3. Infrared Spectroscopy	817
	4. Diffuse Reflectance Spectroscopy	817
	C. Structural	817
	1. X-ray Methods	817
	2. Neutron Methods	818
	D. Microscopic Experiments	819
	1. TEM	819
	2. STM, AFM	819
	E. Thermal Studies	819
	1. TPD Methods	819
	2. Transient Kinetics	820
IV.	Applications	821
	A. Catalysis	821
	B. Photochemistry	822
	C. Electrochemistry	823
V.	Conclusions	823
VI.	Acknowledgments	824

I. Introduction

This review is divided into three major areas in the field of zeolitic and layered materials, including synthesis, characterization, and applications. The focus of the synthetic section concerns new procedures and resultant microporous materials that have three-dimensional and two-dimensional structures. The characterization section is subdivided into magnetic, optical, structural, microscopic, and thermal methods of analysis. The final section concerns three different applications including catalysis, photochemical, and electrochemical applications. While these applications are not all inclusive with regard to recent developments in the area of zeolitic and layered materials, they are of considerable interest primarily on the basis of the numbers of publications in these areas. This review covers the period primarily from about 1989 through 1991. The conclusion section will focus on some of the most recent results in the above-mentioned areas with the thought that these are indicators of future research efforts. Table 1 includes references to books and review articles that can be consulted for background material regarding zeolitic and layered materials.

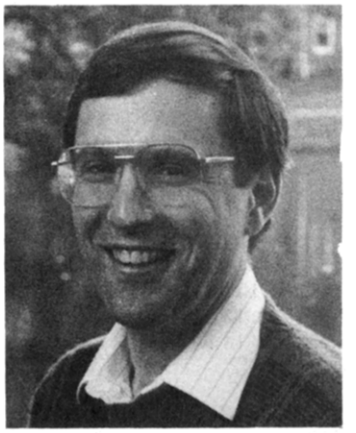

Steven L. Suib received his B.S. degree in chemistry and geology (double major) from the State University College of New York at Fredonia in 1975 and his Ph.D. in Chemistry from the University of Illinois at Champaign-Urbana in 1979 under Professor Galen D. Stucky. After 1 year as a postdoctoral associate with Prof. Larry R. Faulkner at the University of Illinois, he joined the faculty of the University of Connecticut, obtaining the rank of Professor in 1989. His research interests include solid-state inorganic chemistry, heterogeneous catalysis, spectroscopy, and materials chemistry.

II. Synthesis

This section is divided into two separate discussions of zeolites and layered materials.

A. Three-Dimensional Materials

1. New Materials

One of the longterm goals of research in zeolites has been preparation of large single crystals. Klemperer and co-workers[1,2] have recently reported the preparation of large 3-mm size crystals of the ZSM-39 structure type or dodecasil-3C. Thermal, structural, and morphological properties were the primary focus of this work although weak second harmonic generation was also observed. This research represents an important breakthrough in the pursuit of large zeolite crystals.

Since the reports of aluminophosphates,[3] silicoaluminophosphates,[4] and metalloaluminophosphate[5] molecular sieves and the report of the large-pore 18-ring channel VPI-5[6] material, considerable activity is apparent in the preparation of new zeolitic materials. Many of these newly reported materials are phosphorus

0009-2665/93/0793-0803$12.00/0

Table 1. Background Material on Zeolitic and Layered Materials

topic	reference
general	Rabo, J. A., Ed. *Zeolite Chemistry and Catalysis*; ACS Monograph Series 176; American Chemical Society: Washington, DC, 1976.
zeolite synthesis	Barrer, R. M., *Hydrothermal Chemistry of Zeolites*; Academic Press: New York, 1982.
zeolites, clays, adsorption	Barrer, R. M. *Zeolites and Clay Minerals as Sorbents and Molecular Sieves*; Academic Press: London, 1978.
zeolite synthesis	Occelli, M. L., Robson, H. E., Eds. *Zeolite Synthesis*, ACS Symposium Series 398; American Chemical Society, Washington, DC, 1989.
clays	Occelli, M. L., Robson, H. E., Eds. *Expanded Clays and Other Microporous Solids*; Van Nostrand Reinhold: New York, 1992.
clays and layered materials	Clearfield, A. *Chem. Rev.* **1988**, *88*, 125–148.
molecular sieves	Occelli, M. L., Robson, H., Eds. *Molecular Sieves*; Van Nostrand Reinhold: New York, 1992.
structures of molecular sieves	Smith, J. V. *Chem. Rev.* **1988**, *88*, 149–182.

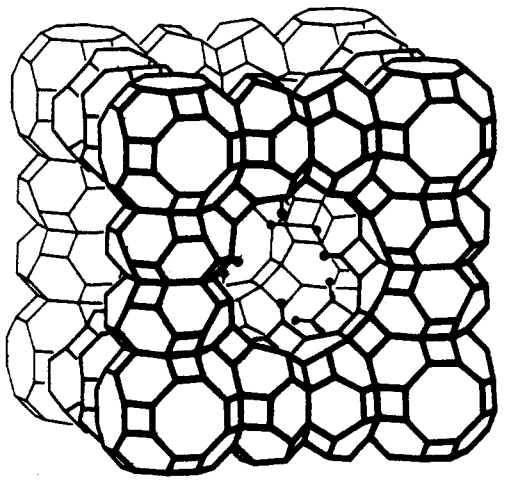

Figure 1. Framework structure of cloverite. Each of the tetrahedral intersections represent either a Ga or P atom bridged by O atoms. The solid circles in this represent some of the terminal hydroxyl groups. Reprinted from ref 7. Copyright 1991 Nature.

based. For example, a 20 tetrahedral atom gallophosphate material having a four-leaf-clover-shaped pore opening nicknamed cloverite has recently been reported.[7] The structure of cloverite is shown in Figure 1. The large interior supercage has a body diagonal dimension of up to 30 Å and is believed to contain hydroxyl groups in the framework. A single crystal refinement of the structure of cloverite has led to the space group $Fm\bar{3}c$ while the organic template was not yet located. Cloverite has been reported[7] to be stable to temperatures of at least 700 °C where a phase change occurs and has been used for sorption of hydrocarbons.

A new series of zinco(beryllo)phosphate and -arsenate molecular sieves isostructural to zeolites RHO, X, and LiA has been prepared at temperatures as low as 70 °C by Stucky and co-workers.[8-11] These materials appear to be more stable than related aluminophosphates and large crystals can be obtained.[12] The structure of a zinc phosphate molecular sieve containing one-dimensional 8-ring channels along the *a* axis is shown in Figure 2. Organic templates have been used to prepare such materials with resultant channels having dimensions 3.5 × 5.0 Å. A tendency to force tetrahedral coordination in these systems is in contrast to related materials having octahedral geometries.

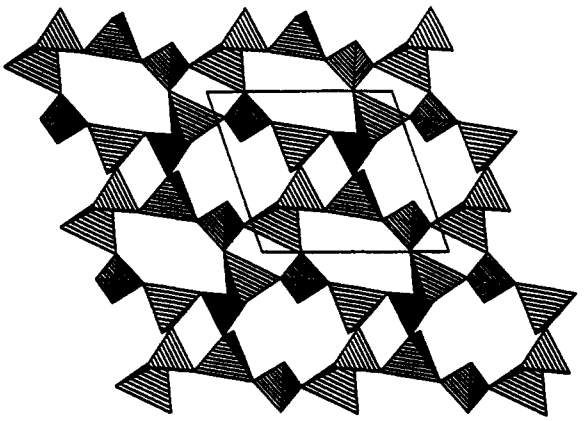

Figure 2. Zinc phosphate 8-ring channels along the a crystallographic direction. Linkages of alternating tetrahedra of Zn- and P-linked via edge sharing O atoms. Reprinted from ref 12. Copyright 1991 American Chemical Society.

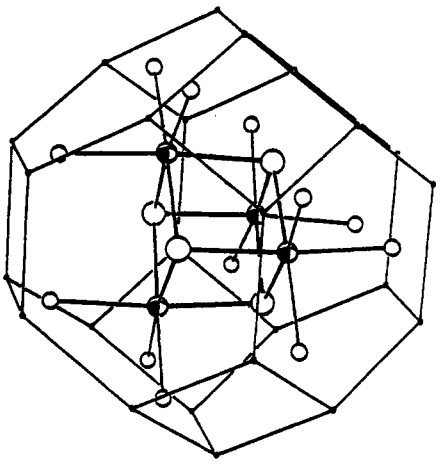

Figure 3. $Na_3(H_2O)_4$ cubane cluster in ZnAsO sodalite structure. Na ions are shaded, framework O atoms are small spheres, O of H_2O are large spheres. The encompassing cage structure shows alternating Zn and As atoms. (Bridging O atoms are omitted.) Reprinted from ref 11. Copyright 1991, ACS.

The structures of new zincophosphate and beryllophosphate systems with the zeolite X structure have been characterized by both X-ray and neutron diffraction methods and are the first examples of zeolite materials consisting of only group IIb atoms.[10] Similar materials having the sodalite structure of open frameworks consisting of either zinc phosphate or zinc arsenate compositions have been prepared at room temperature and yield highly crystalline materials. Rietveld refinement of the zinc arsenate system[11] leads to a cubane geometry of $Na_3(H_2O)_4$ clusters centered in the sodalite cage as shown in Figure 3. These structures are unique and suggest that such novel nonaluminosilicate systems may lead to several other new molecular sieve systems with interesting structures.

Cationic diazabicyclo[2.2.2]octane (DABCO) can be used as a template for novel anionic zinc phosphate 8-ring framework structures.[12] Both zinc and phos-

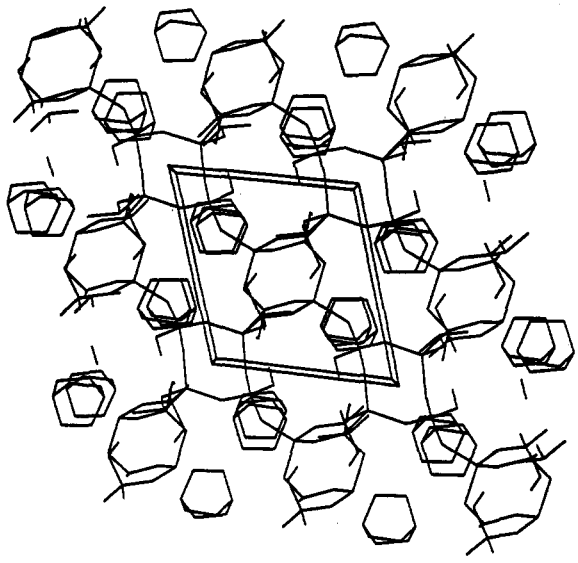

Figure 4. Structure of zinc phosphate including DABCO $[(H_2N_2C_6H_{12})^{2+}]$ template (small interlocked 6-member rings). View down the *a* direction indicating the corrugated 8-ring channels. Reprinted from ref 12. Copyright.

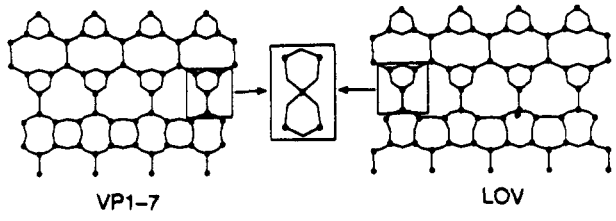

Figure 5. Framework topologies of VPI-7 (zincosilicate) and lovdarite (beryllosilicate). Reprinted from ref 13. Copyright 1991 Royal Society of Chemistry.

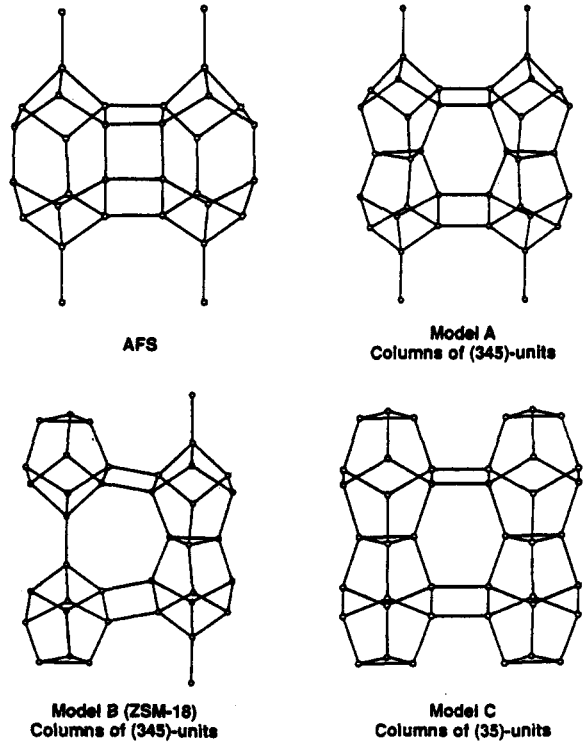

Figure 6. Basic building blocks for ZSM-18. Reprinted from ref 14. Copyright 1990 American Association for the Advancement of Science.

phorus are tetrahedral in such structures which also contain H_2O and OH groups. The channels in such

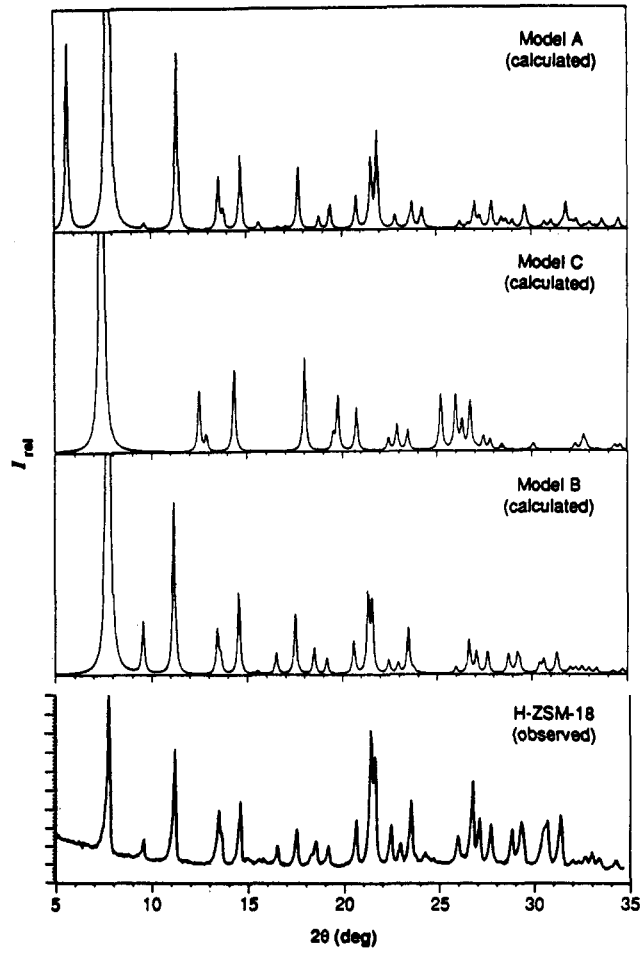

Figure 7. Experimental and theoretical X-ray powder diffraction patterns. Models A–C are theoretical, and H-ZSM-18 is experimental. Reprinted from ref 14. Copyright 1990 American Association for the Advancement of Science.

materials are one-dimensional in nature with thermal stabilities up to 350 °C depending on structure and composition. A complete view down the a direction of the crystal structure of the most thermally stable derivative, ZnPO/Dab-A, with DABCO molecules (small ring structures) present in channels that have a corrugated structure, is shown in Figure 4. The tendency to form this tetrahedrral structure is directly related to the specific choice of template (DABCO).

There has clearly been a move in this field to non-aluminosilicate molecular sieves, such as the phosphate systems described above, which has led to several novel structure types and compositions. Another example includes the novel zincosilicate molecular sieve with three member rings, VPI-7.[13] VPI-7 is related to the mineral lovdarite (beryllosilicate) and can be envisioned as a lovdarite structure with translations along the mirror planes that bisect alternating 4- and 6-member rings of both the 010 and 100 faces as depicted in Figure 5. A novel 3-ring aluminosilicate structure ZSM-18 having the primary building units shown in Figure 6 has also been reported by Lawton and Rohrbaugh.[14] Theoretical X-ray powder diffraction patterns have been calculated for this system as shown in Figure 7 that help confirm the overall structure of H-ZSM-18. Refinement was done with crystallographic parameters on the basis of model B, due to the closeness of theoretical data to experimental data of H-ZSM-18, as shown in Figure 7. Such crystallographic modeling

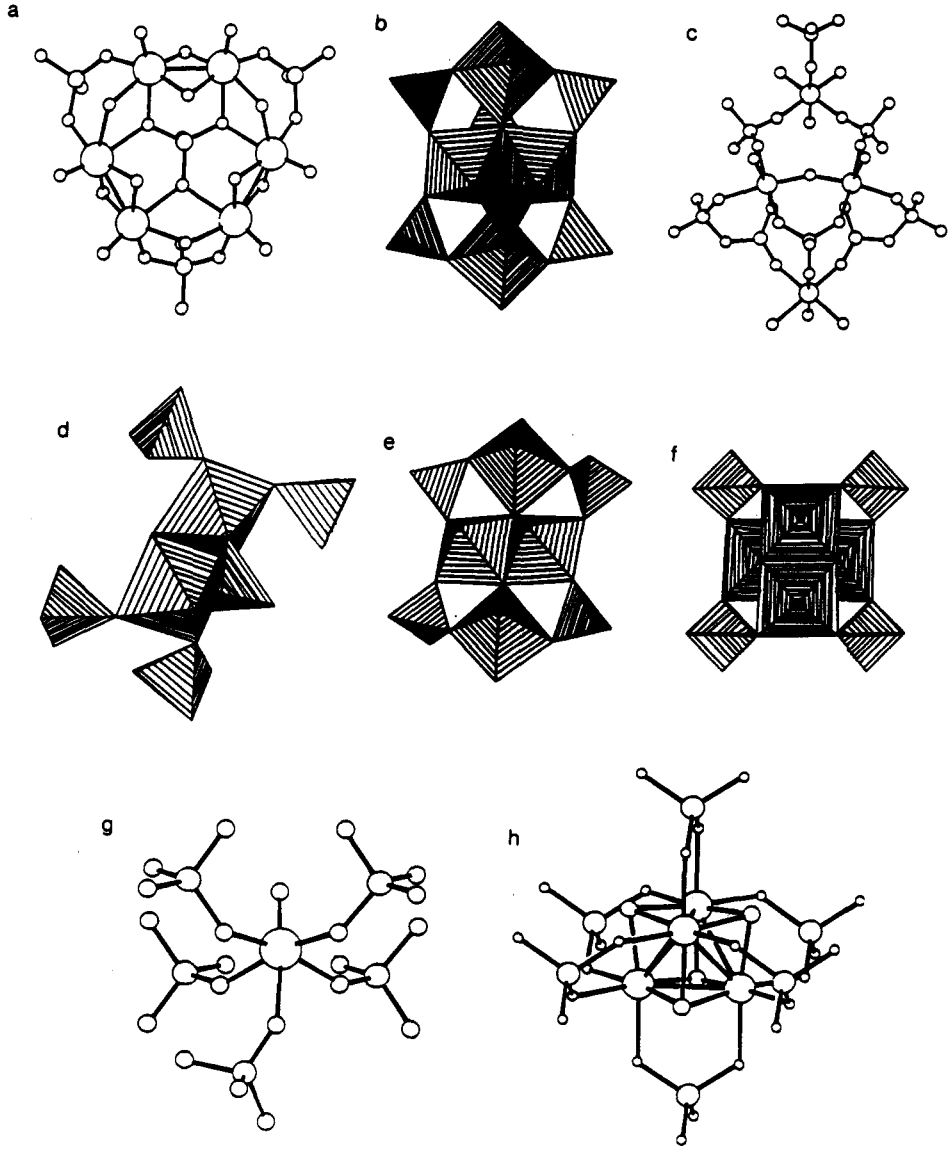

Figure 8. Primary building blocks for reduced molybdenum phosphates: (a) $[Mo_6O_{15}(HPO_4)(H_2PO_4)_3]^{5-}$, (b) $Mo_8O_{12}(PO_4)_4(HPO_4)_2 \cdot H_2O$, (c) O_5MoOMo_5, (d) $Mo_2O_4(HPO_4)(PO_4) \cdot 2H_2O$, (e) Mo_4, (f) Mo_4O_8, (g) $MoO(PO_4)$, (h) $[Mo_4O_8(PO_4)_{4/2}]^{2-}$. Reprinted from ref 15. Copyright 1991 American Chemical Society.

experiments have been used in several of the above mentioned studies.[12-14] These procedures are essential for confirming the presence of new phases.

A new family of microporous molecular sieves consisting of reduced molybdenum phosphates has been reported by Haushalter and co-workers.[15] These materials usually have Mo–Mo bonds, are based on both tetrahedral and octahedral geometries for molybdenum, and have close to 40% accessible void volume. Several structural types have been reported with primary building blocks as depicted in Figure 8. An example of a reduced cesium molybdenum phosphate having a super cube structure is given in Figure 9. This structure is fascinating because it is an example of an octahedral/tetrahedral (Mo/P) interlinked structure which has a void in the center of the cube. This is unique for a material produced at high temperature (950 °C). Several other novel porous structures have been reported by this group[15] consisting of three-dimensional, layered, and polymeric materials. One area of interest that affects possible future research directions concerns the pore windows that are open to the external surfaces of such materials. They are relatively small and thus limit applications for sorption and catalysis.

There may be several phases that are accessible with phosphate molecular sieves. Considerable debate has recently ensued concerning 18 ring aluminophosphate systems such as VPI-5, H1, and related materials. The synthesis of H1 via amine templates has recently been reported,[16] and its structure has been determined from synchrotron X-ray powder diffraction data. The presence of amine template and the observation of 6 coordinate aluminum has been suggested by Clearfield and co-workers[16] for H1. Tributylamine templates are observed in the pores of H1 as is shown in Figure 10, and 6 coordinate aluminum species are believed to be part of the double 4 member rings. On the other hand, synthesis of H1 without organic templates has also been reported.[17]

Octahedral molecular sieves have also recently been reported. Tunnel structures of titanium, in particular those such as $Na_2Ti_6O_{13}$, have been shown to be useful photocatalysts for decomposition of water.[18] Related manganese oxide tunnel structure materials similar to

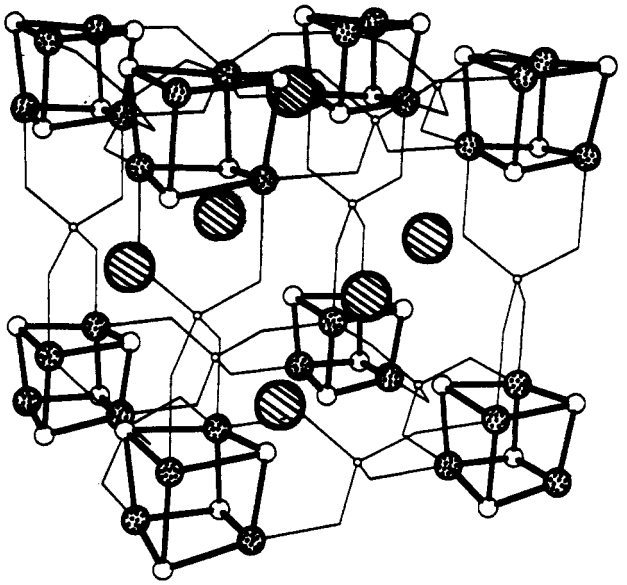

Figure 9. Mo_4O_4 cubes of $Cs_3Mo_4P_3O_{16}$. Cs ions are represented by striped spheres; P atoms are small open spheres; Mo are dotted spheres; Cs ions are located in the face centers of the cube, P at the edges. Reprinted from ref 15. Copyright 1991 American Chemical Society.

the mineral todorokite have been reported[19] by our group in collaboration with researchers at Texaco, Inc. The structure of an octahedral molecular sieve (OMS-1) having a 3 × 3 MnO_6 framework giving rise to 1 dimensional tunnels having a pore dimension of 6.9 Å is shown in Figure 11. It is not clear why manganese systems allow this particular structure, which is believed to exist in manganese nodules; however, it may be related to the ability of manganese to exist in octahedral coordination for a multitude of oxidation states (2+ – 4+).

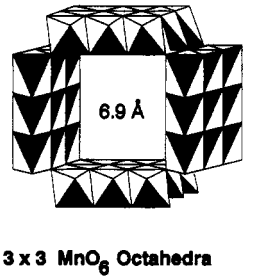

Figure 11. Structure of octahedral molecular sieve 1, OMS-1. MnO_6 octahedral units are linked via edges and vertices. Pore diameter is 6.9 Å. Reprinted from ref 19. Copyright 1992 Royal Society of Chemistry.

Other procedures for preparation of microporous three-dimensional materials include pillaring of layered systems such as clays.[20] A recent development in this area involves the pillaring of a natural clay rectorite with polyoxo cations of aluminum and zirconium/aluminum by Guan and co-workers.[21] Similar materials

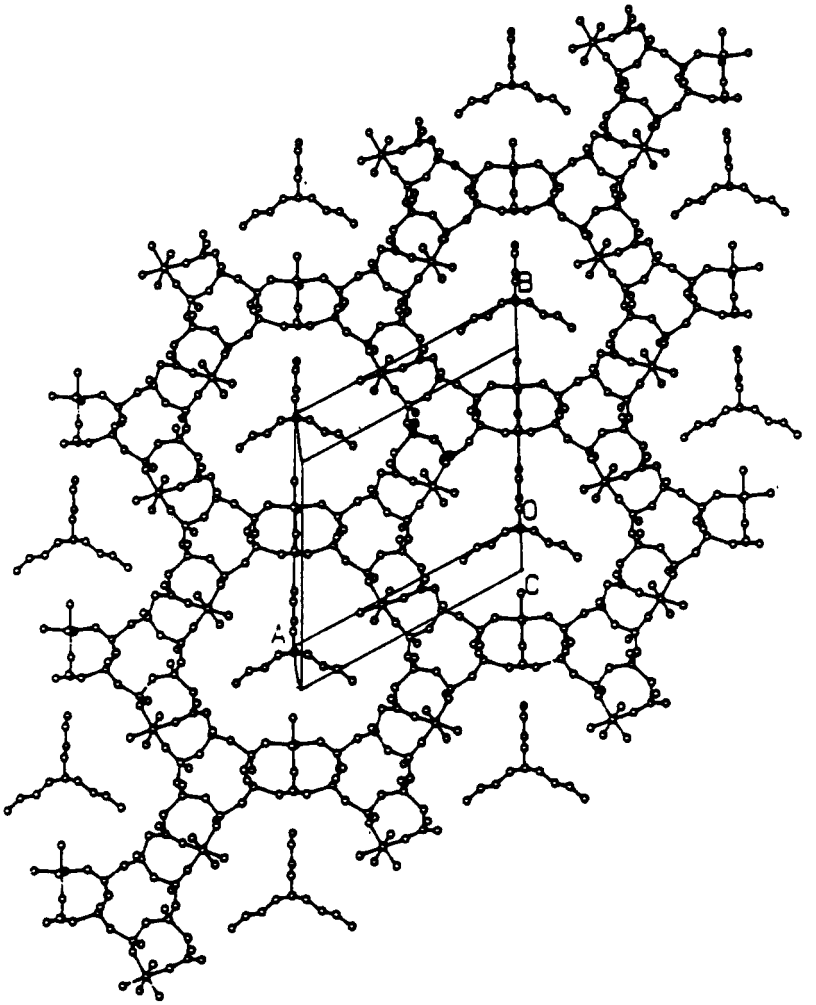

Figure 10. Structure of H1 showing 6-coordinate Al in the double 4-member rings and tributylamine template centered in the 18-membered rings. Reprinted from ref 116. Copyright 1991 Baltzer.

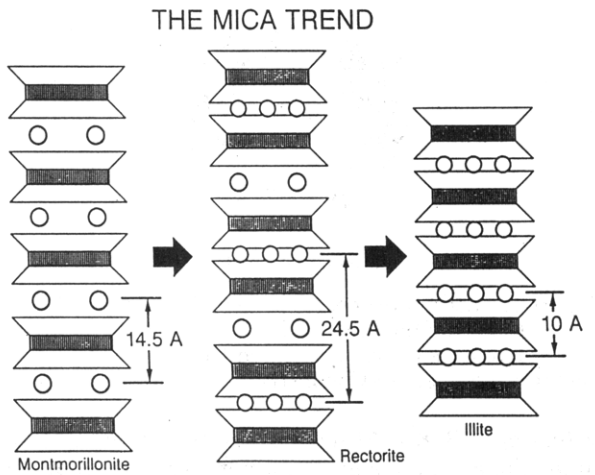

Figure 12. Comparative structures of montmorillonite, rectorite, and illite having two, three, and one molecular water layers, respectively. Trapezoids represent tetrahedral coordinated layers; striped rectangles represent octahedral layers; spheres represent interlayer water molecules. Reprinted from ref 22. Copyright 1991 Elsevier.

have been prepared by Occelli[22] who has compared the basic repeat units for a clay that has more often been pillared, montmorillonite, and a natural clay (illite) to that of rectorite as shown in Figure 12. The difference between these three materials is the degree of interlayer water which controls the d spacing as summarized in Figure 12. Some of the interlayer cations of rectorite are not exchangeable. An interesting observation of these materials is that they are stable after calcination to 800 °C and after steam aging at 760 °C. This has not been generally found to be the case for other pillared clay systems.

Other layered systems that recently have been shown to be able to be pillared include vanadium oxide[23] (by Mo_6 and Nb_6 halohydroxy cations) and buserite[24] a layered magnesium octahedral manganese oxide. The buserite system was pillared by first propping open the layers with an organic moiety (*n*-hexyl ammonium cations) and then using polyoxocations of aluminum to pillar the buserite. This basic two-step procedure for pillaring was first introduced by Drezdon.[25] Another relatively recent approach has been the substitution of trivalent ions for Al^{3+} ions in the polyoxoaluminum cations, such as work of Sterte where La^{3+} ions were incorporated into aluminum oligomers.[26]

2. Isomorphous Substitution

Another major emphasis in synthesis of zeolites has been isomorphous substitution of trivalent ions into zeolitic frameworks usually to replace Al^{3+} ions. The systems that have been studied the most include Fe^{3+}, B^{3+}, and Ga^{3+}. Reviews of research from particular groups are available;[27-30] however, most studies have concerned substitution of one of the above-mentioned trivalent ions. The focus of most of these studies has been either use of such systems in catalytic reactions or characterization of the isomorphously substituted ion, and therefore will be discussed in other sections of this review.

Gallium-substituted zeolites have been the focus of several researchers in recent years. The amount of Ga(III) incorporated into various zeolite frameworks

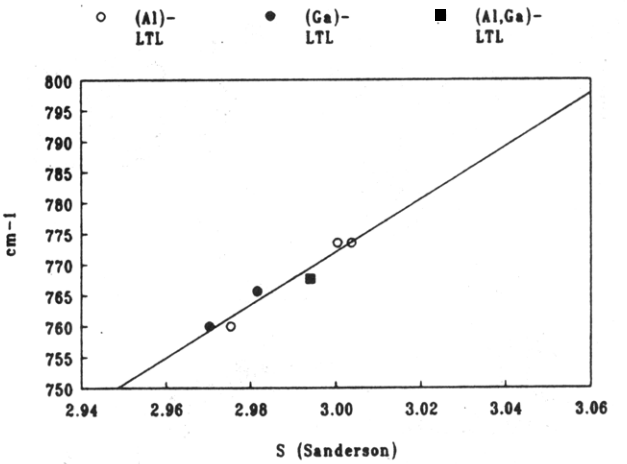

Figure 13. Frequency of T–O stretching vibration versus Sanderson electronegativity for LTL (Linde type L) zeolites: (○) Al LTL; (●) Ga LTL, (■) Al,Ga LTL. Reprinted from ref 31. Copyright 1991 Academic.

appears to be correlated to a shift in the asymmetric stretching vibration of internal tetrahedra of gallosilicates having the faujasite, L, β and ZSM-5 structure. Framework Ga LTL zeolites have been studied with infrared spectroscopy recently,[31] and correlations have been found between framework vibrations and the electronegativity of Ga in the framework. Figure 13 shows a plot of frequency of the symmetric stretching vibration for external linkages of Al, Ga and Al,Ga LTL zeolites as a function of Sanderson electronegativity. Excellent correlations with Sanderson electronegativity for other bands such as asymmetric stretching vibrations of internal tetrahedra were also observed. This correlation is important from a synthetic standpoint since it may be possible to predict the extent and possibility of Ga(III) substitution in molecular sieves on the basis of electronegativity principles.

A variety of materials having boron substitution in the ZSM-5 structure have been reported by Cichocki et al.[32] The major emphasis of this research was to determine synthetic conditions that might control the extent of isomorphous substitution. These authors[32] suggest that the most important parameter is the ratio of SiO_2/B_2O_3 in the synthesis mixture; however, impurities of Al^{3+}, Ti^{4+}, and Fe^{3+} were important for low levels of B^{3+} substitution.

A final example of novel approaches to prepare molecular sieves includes synthesis of zeolite A where the reactant species were enclosed in reverse micelles by Dutta and Robins.[33] It is not apparent how nucleation and crystallization phenomena are influenced by this type of procedure although gravitational forces were not avoided by use of the micelles.

B. Layered Materials

Inorganic ion-exchange materials have been the focus of a recent review;[34] however, several recent developments in the area of synthesis are apparent since this time. Porphyrins and metalloporphyrins have recently been used during hydrothermal crystallization of layered silicate smectite clays by Carrado and co-workers.[35,36] Structures of the porphyrin molecules used in these gel syntheses are shown in Figure 14. Such materials can be prepared in a relatively short period

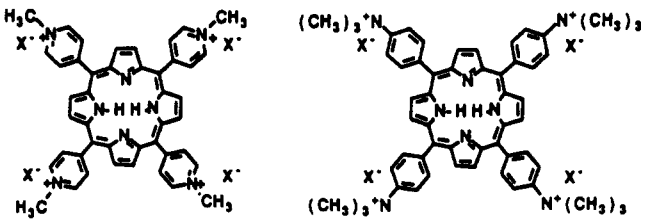

TMPyP TAP

Figure 14. Porphyrin intercalates for hectorite: TMPyP, tetrakis(*N*-methyl-4-pyridiniumyl)porphyrin; TAP, tetrakis-(*N,N,N*-trimethyl-4-aniliniumyl)porphyrin. Reprinted from ref 35. Copyright 1991 American Chemical Society.

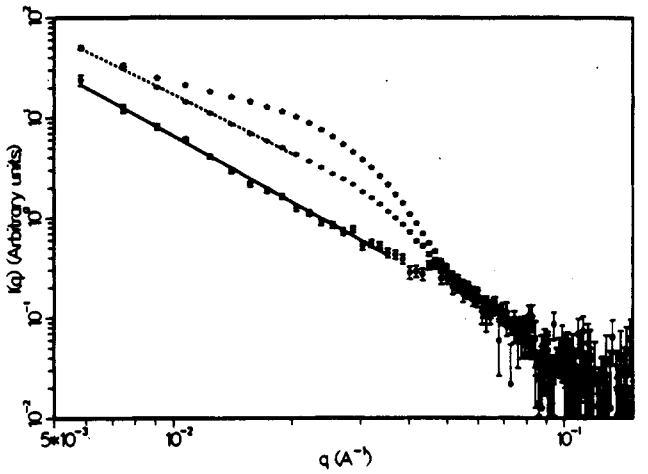

Figure 15. Plot of log intensity versus log q of small angle neutron scattering (SANS) for TMPyP (see caption for figure 14) hectorite clay system: (○) hectorite, (△) unheated TMPyP-Hectorite Gel, (+) TMPyP–hectorite gel refluxed. Reprinted from ref 35. Copyright 1991 American Chemical Society.

of 2 days during which small angle neutron scattering (SANS) experiments were done to follow the nucleation process.[35]

SANS data for hectorite, the unheated porphyrin hectorite gel, and the heated (refluxed) porphyrin hectorite gel show that the intensities for scattering versus the inverse of the wave vector of Figure 15 are markedly different.[35] The shapes of these curves suggest a lamellar structure for the hectorite control sample, aggregation for the unheated porphyrin hectorite gel and finally a decrease in the middle q region for the heated porphyrin gel system. These data indicate that aggregates present in the unheated gel are dispersed on thermal treatment and give rise to interdispersed porphyrin/hectorite layers. These and other[38] studies suggest that SANS methods are useful for more readily understanding processes that occur in gels during nucleation and crystallization. Future studies with SANS may allow in situ characterization of aggregation processes for molecular interactions in gels and related media.

Fluorohectorite has recently been intercalated with aniline to produce polyaniline by Mehrotra and Giannelis.[37] On exposure of this material to HCl vapor, conductivities of 0.05 s cm^{-1} were realized. A plot of log in-plane conductivity versus $T^{1/2}$ is given in Figure 16 for the polyaniline intercalated fluorohectorite sample. These studies suggest that the conductivity is

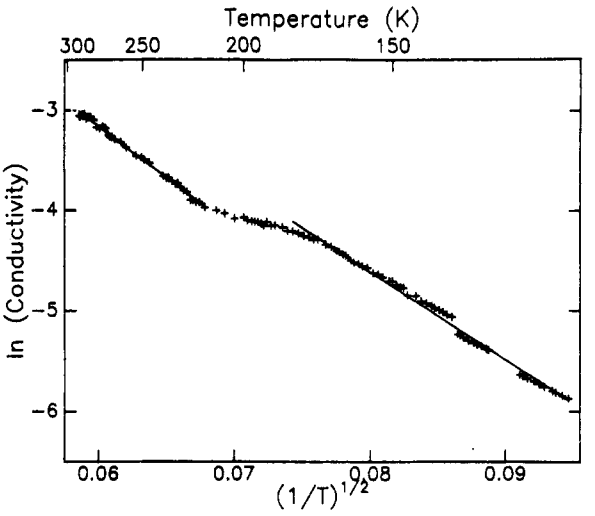

Figure 16. log in-plane conductivity versus $T_{1/2}$ for polyaniline silicate multilayers for aniline polymerized in fluorohectorite clay. Reprinted from ref 37. Copyright 1991 Pergamon.

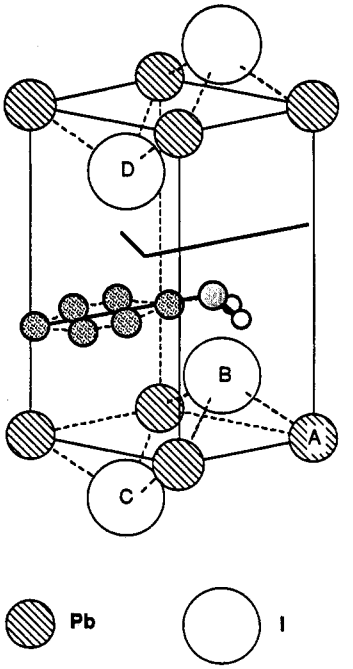

Figure 17. Structure of PbI_2 aniline intercalate. Interactions between different ions and A–D between different unit cells is necessary to explain conductivity. Intercalated aniline is shown inside the unit cell of PbI_2. Reprinted from ref 39. Copyright 1991 American Institute of Physics.

structure dependent; the transverse conductivity was 5 orders of magnitude lower than the in-plane conductivity. Such data imply that conductivity of similar systems may be fine tuned by engineering the molecular structure of intercalated materials.

Giannelis et al.[39] have also reported that aniline can be intercalated into the layered PbI_2 structure as is shown in Figure 17. The band gap of the intercalated PbI_2 system was changed by about 0.5 eV as shown in the optical data for the unintercalated and intercalated systems as shown in Figure 18. These systems are excellent examples of how optical and electrical properties can be controlled in intercalated layered materials by wise choices of types and concentrations of intercalate.

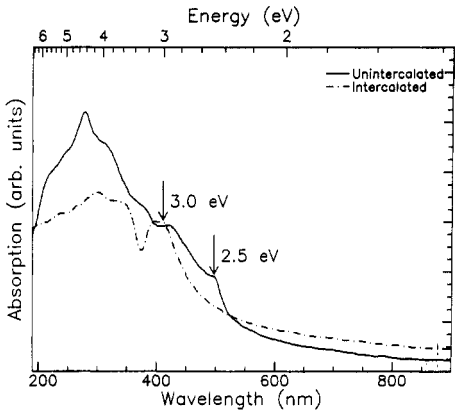

Figure 18. Optical spectra for PbI_2 and aniline intercalated PbI_2. Reproduced from ref 39 with permission.

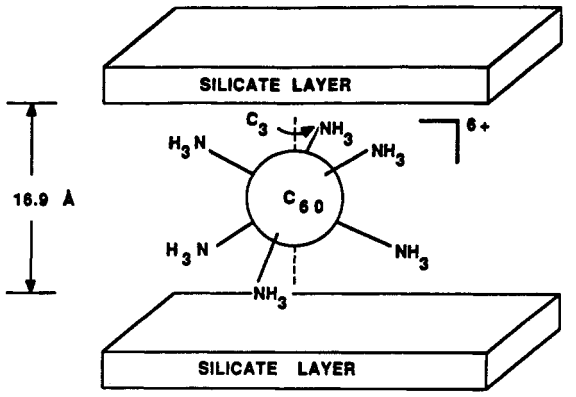

Figure 19. Structure of ethylenediamine-functionalized C_{60} in fluorohectorite. Reprinted from ref 40. Copyright 1992 American Chemical Society.

A final example of intercalated micas involves insertion of ethylenediamine-functionalized buckminsterfullerene (C_{60}-EDA) into fluorohectorite.[40] Thermal studies show that the resulting materials are stable up to at least 800 °C, depending on the atmosphere used during heat treatment. A model of the structure of this intercalated system is shown in Figure 19 which is consistent with X-ray diffraction data reported for this system. This is one of the first examples of incorporation of buckeyball materials into zeolitic and layered materials. It is likely that other oxide materials based on these new carbon cluster systems will be forthcoming.

Layered phosphonate systems are also flexible microporous solids that have been the subject of great interest in recent years. A major advantage of these systems over several zeolitic and layered materials is that single crystals can be prepared and studied by single-crystal X-ray diffraction methods. A packing diagram for $Ca(O_3PCH_3)\cdot H_2O$ depicting the representative layered structure of such materials and a unit cell are shown in Figure 20 for one such system studied by Mallouk and co-workers.[41] A comparison of idealized structures of Ca, the more commonly studied Zr and lanthanum phosphonate systems was recently proposed and depicted in Figure 21.

Similar phosphonate systems can be dehydrated to yield anhydrous salts that can adsorb various amines. These produce different types of structures that have been referred to as shape-selective intercalates[42] as depicted in Figure 22. The exact reasoning as to why some systems prefer single layers and others double

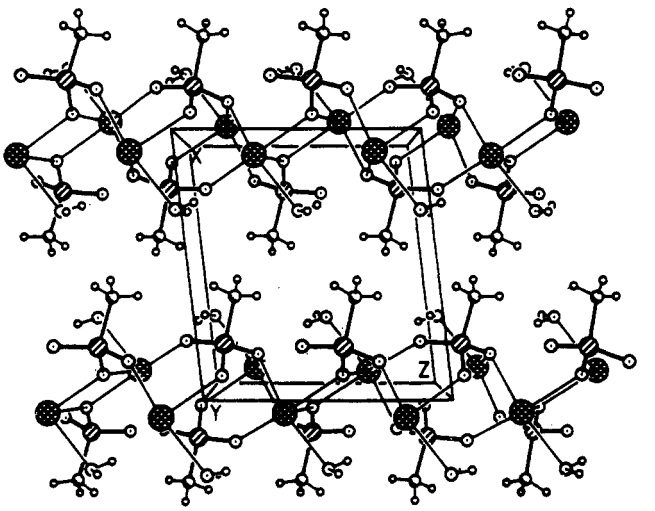

Figure 20. Structure of $Ca(HO_3PC_6H_{13})_2$ showing the layered nature and A unit cell. Ca ions are large hatched spheres; P atoms are small striped spheres; open spheres with dot in middle are O ions. Reprinted from ref 41. Copyright 1990 American Chemical Society.

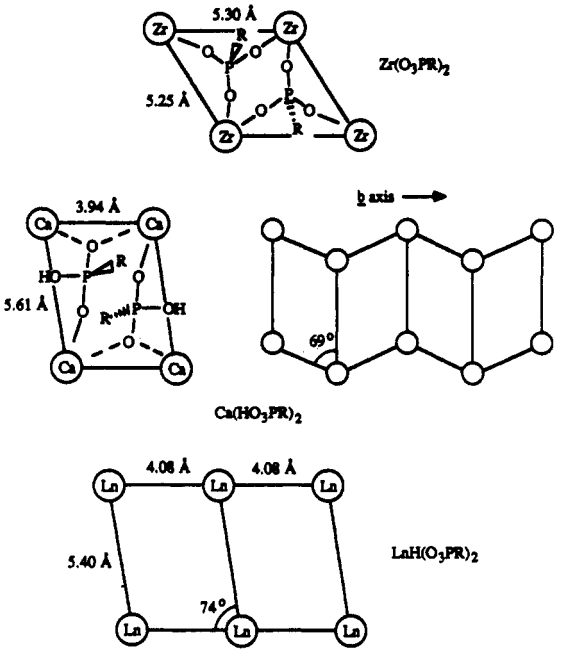

Figure 21. Ideal structures for $Ca(HO_3PR)_2$, $Zr(O_3PR)$, and $LaH(O_3PCH_3)_2$. Reprinted from ref 41. Copyright 1990 American Chemical Society.

layers may involve steric factors. If a particular structure type could be controlled or predicted, several applications of resultant materials would likely be found. A comparison of layered phosphonates to other two- and three-dimensional systems has been made with the suggestion that the layered phosphonates are good models for surfaces.[43]

In fact, the tethering of phosphonates to solid surfaces such as silica has been the most recent focus of much research concerning phosphonates by Mallouk and coworkers.[44] A general scheme for the anchoring of phosphonates to a cab-o-sil surface is depicted in Figure 23. Mixed phosphonate and phosphate materials were also prepared with similar methods. Anchoring of phosphonates and similar moieties to surfaces can lead to stable robust surfaces for catalytic, electrochemical and photochemical studies. It is also often relatively

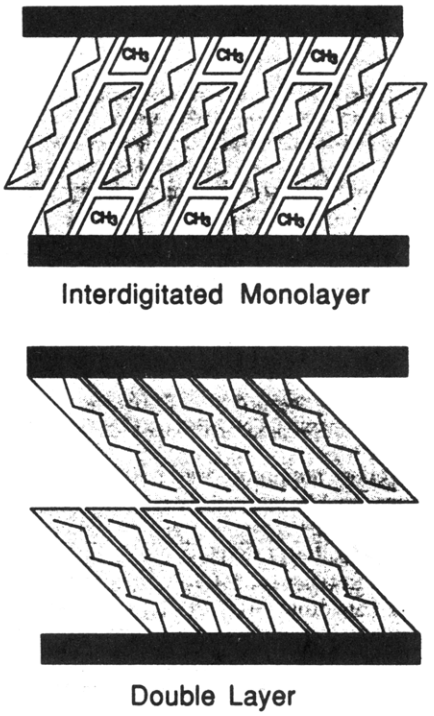

Figure 22. Interdigitated mono and double layer alkyl chains of amine intercalated $M(O_3PCH_3)$. Amines like NH_3, methylamine, *n*-heptylamine, and others can be intercalated. Reprinted from ref 42. Copyright 1991 American Chemical Society.

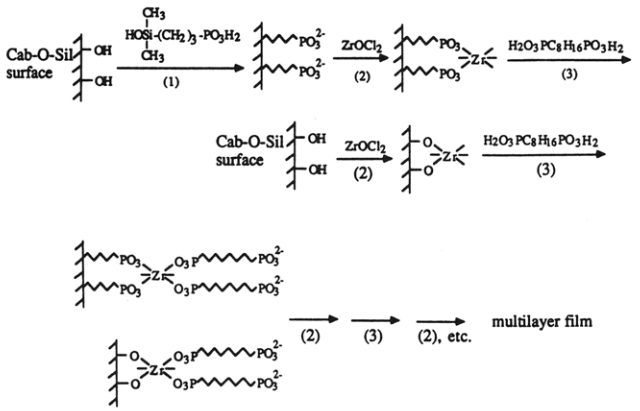

Figure 23. Scheme for growth of zirconium bisphosphonate films on Cab-O-Sil. Reprinted from ref 44. Copyright 1991 American Chemical Society.

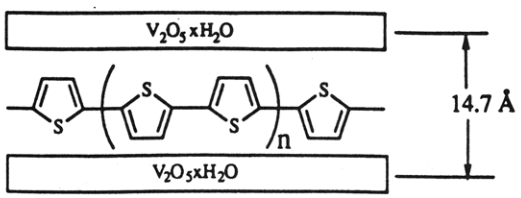

Figure 24. Structure of bithiophene intercalated vanadia. Reprinted from ref 47. Copyright 1990 American Chemical Society.

easy to characterize such systems as compared to other surface deposition methods because certain configurations appear to be favorable and location at the surface is almost always guaranteed.

Layered vanadium oxide, V_2O_5, has also been used for several intercalation studies lately by Kanatzidis and co-workers. Intercalates of polyaniline,[45] pyrrole,[46] and 2,2′-dithiophene[47] in V_2O_5 xerogels have led to a series of conductive polymeric materials. One such intercalate (2,2′-dithiophene) is depicted in Figure 24. Related research on intercalation of poly(ethylene oxide) results in insulating polymers[48] that can be ion-exchanged with lithium and on irradiation with ultraviolet light give rise to materials with conductivities on the order of 10^{-2} s/cm. These are believed to be n-type semiconducting materials.

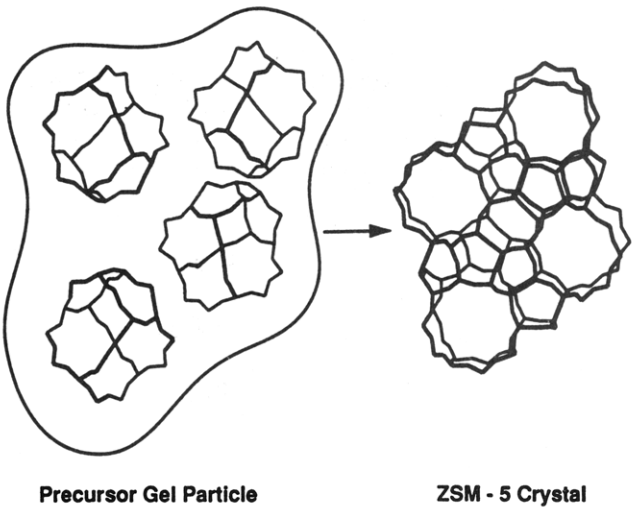

Figure 25. Mechanism for nucleation of ZSM-5 Gels. Reprinted from ref 50. Copyright 1991 Baltzer.

III. Characterization

This section will focus on unique methods of characterization of zeolitic and layered materials. Various sections concerning magnetic, optical, structural, microscopic, and thermal methods will be discussed.

A. Magnetic Methods

1. Nuclear Magnetic Resonance

Reviews of solid-state magic-angle nuclear magnetic resonance studies of zeolites and molecular sieves[49,50] have very recently been reported; therefore, only the most recent applications for these three-dimensional materials will be given. Data from Si NMR on gels of ZSM-5 by Chang and Bell[50] suggest that channel intersections are formed first in the gel. These channels are randomly connected at first and then rearrange to form the ZSM-5 framework structure in a process governed by hydroxyl groups. The general mechanism is shown in Figure 25 and summarized in Scheme 1. It is not clear whether such precursor species are present in other zeolite systems.

Studies of VPI-5 and H1 with NMR methods have been reported by Perez et al.[51] which suggest that the hydration level in these materials can control the interconversion to $ALPO_4$-8. Evidence for 6-coordinate aluminum was also presented.

NMR methods have been used to study Lewis acid phosphine base adducts in zeolite Y by Lunsford and coworkers.[52] The resulting $AlCl_3$–$P(CH_3)_3$ adducts have different stoichiometries and structures. Two structures of the Al–P coordination complexes are given in Figure 26; bond distances determined from NMR are in good agreement with data from X-ray diffraction

Scheme 1

$$R^+ + nH_2O \rightleftharpoons \ldots \rightleftharpoons ch + H^+$$
$$ch + n(Na_xH_{3-x}SiO_4)^- + (n-1)H^+ \rightleftharpoons \ldots \rightleftharpoons cs + [n(2-x)-1]H_2O + nxNa^+ + (nx+1)OH^-$$
$$cs \rightarrow [\equiv SiOH^- OSi\equiv \rightleftharpoons \equiv SiOSi\equiv + OH^-] \rightarrow \text{nuclei}$$

ch = clathrate-like hydrate
cs = clathrate-like silicate
$0 \leq x < 3$

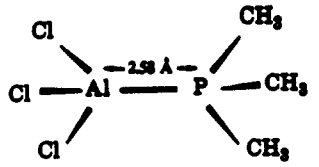

(I)

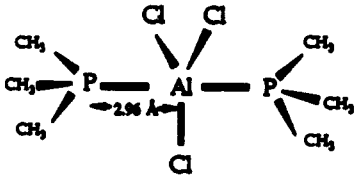

(II)

Figure 26. Two Al–P coordination complexes: $Cl_3AlP(CH_3)_3$ (I) and $(CH_3)_3PAlCl_3P(CH_3)_3$ (II). Reprinted from ref 52. Copyright 1991 American Chemical Society.

studies. An equilibrium between the two structures of Figure 26 is believed to exist.

Various cation-exchanged layered clay vermiculite samples have been investigated by Fripiat and co-workers,[53,54] and NMR results suggest that chemical shifts are directly related to the degree of hydration. Specific factors that control the chemical shifts are lattice interactions, water and oxygen ligands, and the degree of back-donation from ligands to cations. The degree of hydration also strongly influences the quadrupole coupling constant for the case of Cs^+ cations. An excellent correlation between observed chemical shift and the number of oxygen ligands (M) and number of sites available to the cation (N) was found as shown in Figure 27.

Dealumination of vermiculite with $(NH_4)_2SiF_6$ solutions and intercalation of aluminum hydroxy polymers (Al_{13}) was also followed by the NMR methods of Fripiat and co-workers.[54] This system is interesting since no high d spacing was observed on incorporation of the Al_{13} moiety; however, a significant increase in surface area was measured.

Layered silicates that are puckered have also been studied by Si and Al NMR methods by Fripiat and co-workers[55] before and after pillaring with aluminum polyhydroxy polymers. Evidence for octahedral, tetrahedral, and pentacoordinate Al^{3+} species having chemical shifts of 0.4, 56.8, and 33.4 ppm, respectively, was found after calcination at 300 °C as shown in the NMR spectra of Figure 28.

Recent NMR studies of borosilicate gels have been reported from our laboratory in collaboration with researchers at Texaco, Inc.[56] The environment of B^{3+} during nucleation and crystallization of the gel was monitored with B NMR methods. The degree of hydration controlled by the geometry of the B^{3+} species which was determined to be tetrahedral at high levels of hydration and trigonal after extensive dehydration. These NMR results are shown in Figure 29 and will be correlated to optical data presented later in this review.

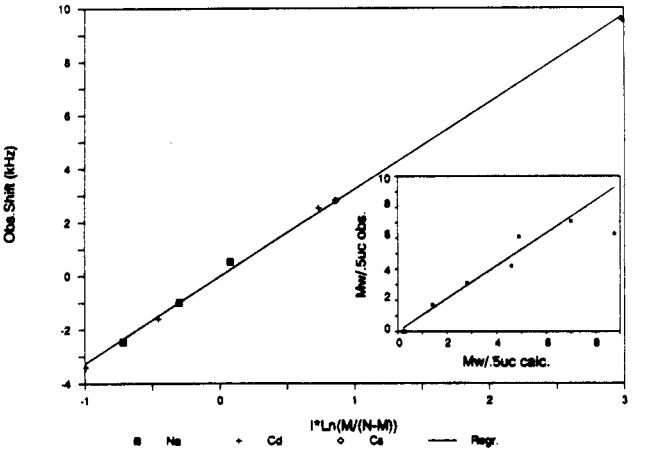

Figure 27. Observed chemical shift versus $I \ln M/(N-M)$, where M stands for M ligands and N is the number of sites. Reprinted from ref 53. Copyright 1990 American Chemical Society.

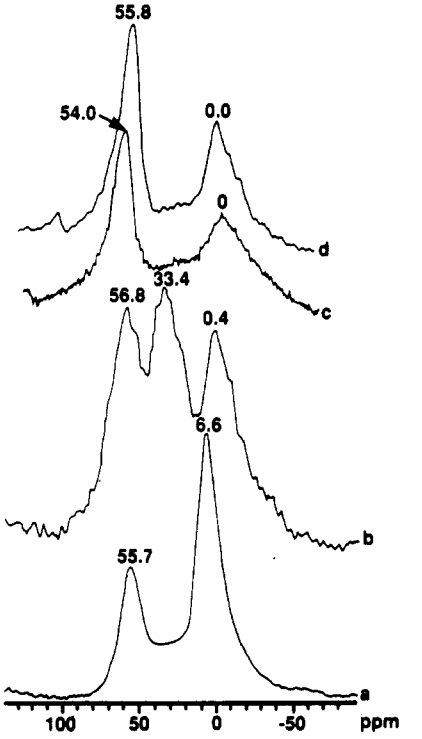

Figure 28. ^{27}Al MASNMR spectrum of pillared puckered silicate sample: (a) direct exchange, (b) sample a calcined 300 °C, 2 h; (c) indirect exchange of ethyl ammonium chloride intercalate; (d) sample of c calcined at 300 °C, 2 h. Reprinted from ref 55. Copyright 1989 American Chemical Society.

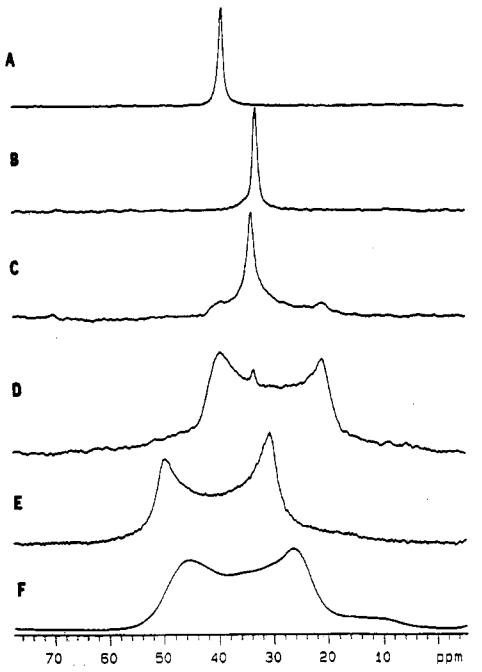

Figure 29. ^{11}B magic angle spinning NMR of (a) B-ZSM-11 sol, (b) B-ZSM-11 gel after 2 days drying, (c) rehydrated crystals of B-ZSM-11, (d) crystallized B-ZSM-11, (e) H_3BO_3, (f) B_2O_3. Reprinted from ref 56. Copyright 1992 American Chemical Society.

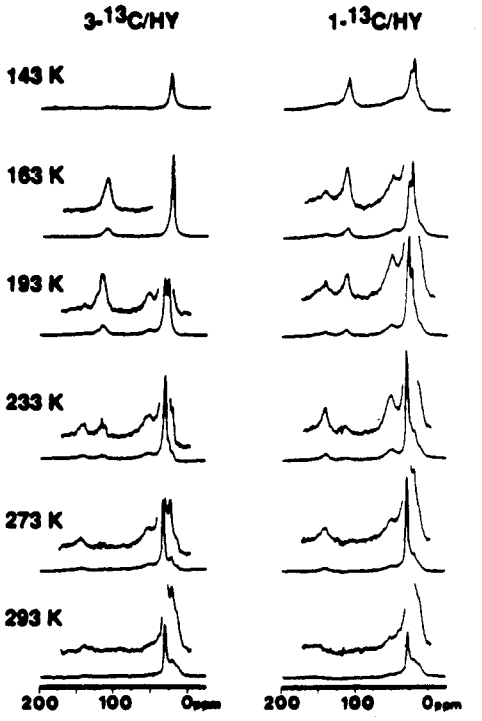

Figure 30. ^{13}C MASNMR spectra of isobutylene-*3*-^{13}C and isobutylene-*1*-^{13}C in HY zeolite. Reprinted from ref 57. Copyright 1991 American Chemical Society.

Haw and co-workers[57] have promoted the use of NMR methods to study acidity in zeolite systems such as HY and HZSM-5. C^{13} CP MAS NMR spectra for the reaction of isobutylene in HY and HZSM-5 are shown in Figure 30. These data suggest that isobutylene dimerizes in both zeolites. However, more dimerization occurs with HY since it has more sites and a downfield shift for the HZSM-5 system suggests that it is more acidic than the HY system. Such in situ measurements

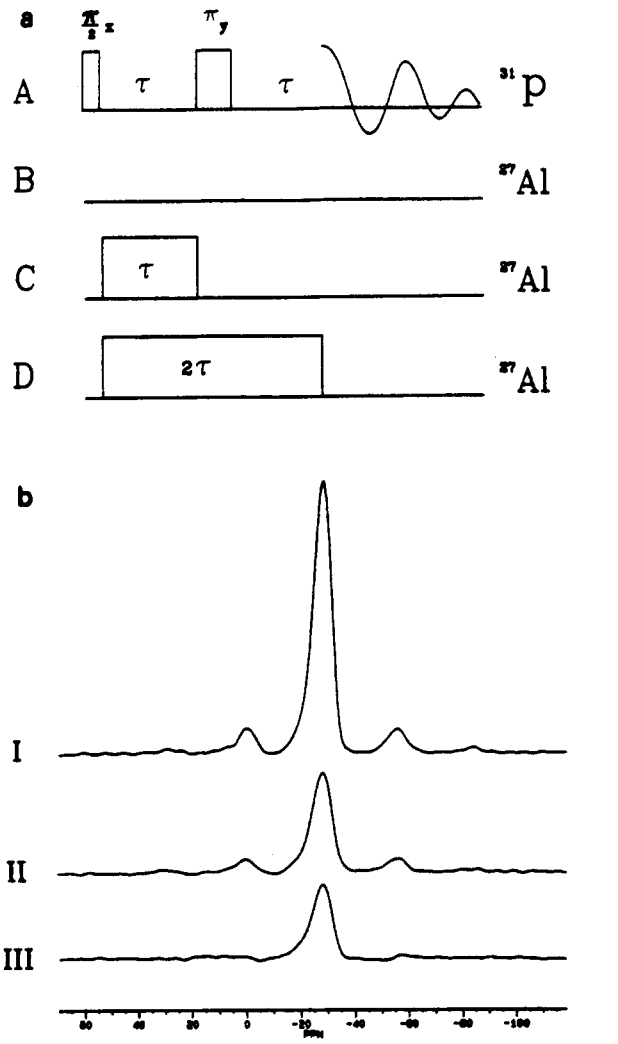

Figure 31. ^{31}P NMR spectra and pulse sequences (I), pulse sequence A and B (II), A and C (III), A and D, having spin echo delay time τ. Reprinted from ref 59. Copyright 1990 Elsevier.

provide information on acid sites that is difficult to obtain by other methods.

Further studies by NMR of acid sites have been done by Hunger, Freude, and Pfeifer[58] on weakly rehydrated dealuminated zeolites. An NMR resonance at 6.5 ppm was assigned to adsorption of water on Lewis acid sites. Evidence for exchange among water molecules, bridging hydroxyl groups, and hydronium ions in zeolites was also postulated on the basis of shifts in the ^1H NMR resonances.

Spin echo NMR data for $ALPO_4$-5 and the different pulse sequences are shown in Figure 31 for experiments done by van Eck and co-workers.[59] Sequences AB, AC, and AD were done with corresponding NMR spectra showing that the ^{31}P and ^{27}Al species are coupled in these materials. Similar experiments were done for NaY zeolite by trying to observe coupling of ^{29}Si and ^{27}Al, but the coupling appears to be miniscule.

2. Electron Paramagnetic Resonance

Electron paramagnetic resonance (EPR) methods are typically used to characterize the environment of paramagnetic ions substituted into either the framework or cation exchange sites of zeolites and clays. A specific example is the EPR investigation of Fe^{3+}

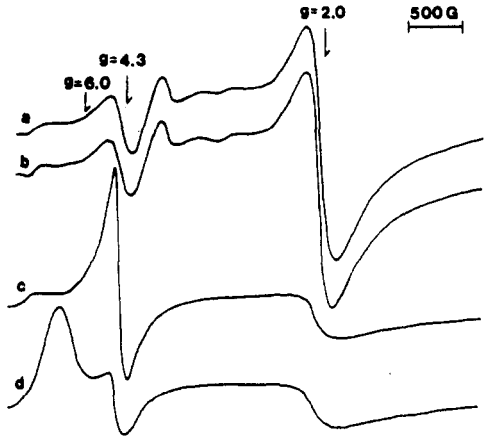

Figure 32. EPR of iron-substituted $ALPO_4$-5: (a) calcined, (b) H_2 treatment at 770 K, 2 d, (c) sample a exposed to H_2O, 24 h; (d) exposed to NH_3 (300 Torr), 30 min. Reprinted from ref 60. Copyright 1992 Academic.

environments in $ALPO_4$-5 materials by Park and Chon[60] as shown in Figure 32. These data suggest that at least two types of Fe^{3+} species are present in these materials, tetrahedral species having $g = 4.3$ and octahedral species with $g = 2.0$.

Schoonheydt and co-workers have pioneered the use of EPR methods to study clays and zeolites and in particular have advocated the combination of diffuse reflectance and EPR methods.[61] Specific examples of such characterization to Cu^{2+}, Ni^+, and Ag cluster systems also including simulated EPR data have recently been given.[61,62] Examples of experimental and simulated spectra for Cu^{2+} A, Y, and X zeolites is given in Figure 33, and the excellent agreement is apparent. Similar studies of the formation of Ni clusters in stages from Ni^{2+} ions to Ni^+ ions to cationic clusters to zerovalent clusters have been reported.[63] Elucidation of several different Cu^{2+} environments in ZSM-5 and mordenite with EPR methods have also been reported.[64,65]

Kevan and co-workers[65] have promoted the use of EPR and electron spin echo methods to study paramagnetic species in zeolites and clays. The rate of growth of the seven-line EPR signal for Ag_4 clusters in A zeolite and that of a five-line EPR signal for Ag_7 in zeolite ρ as a function of reduction time were compared. These data[65] have been used to track the stability of such clusters as a function of time of reduction at room temperature as shown in Figure 34.

By using a combination of EPR and electron spin echo methods, Chen and Kevan[66] have recently determined the structure of Cu^{2+} ions in CuSAPO-5 in water and in methanol as shown in Figures 35 and 36, respectively. Such specific cation–sorbate interactions are generally difficult to pinpoint spectroscopically.

Electron spin echo modulation analyses have also been used to study the incorporation of Mn^{2+} into $AlPO_4$-11,[67] the interactions of CO, NO, O_2 and H_2O with Ru(II) and Ru(III) in HX zeolite,[68] and the environment of silver atoms in sodium montmorillonite before and after pillaring with polymeric hyroxyaluminum species.[69] EPR methods have also been used recently by the same group to characterize the oxidation

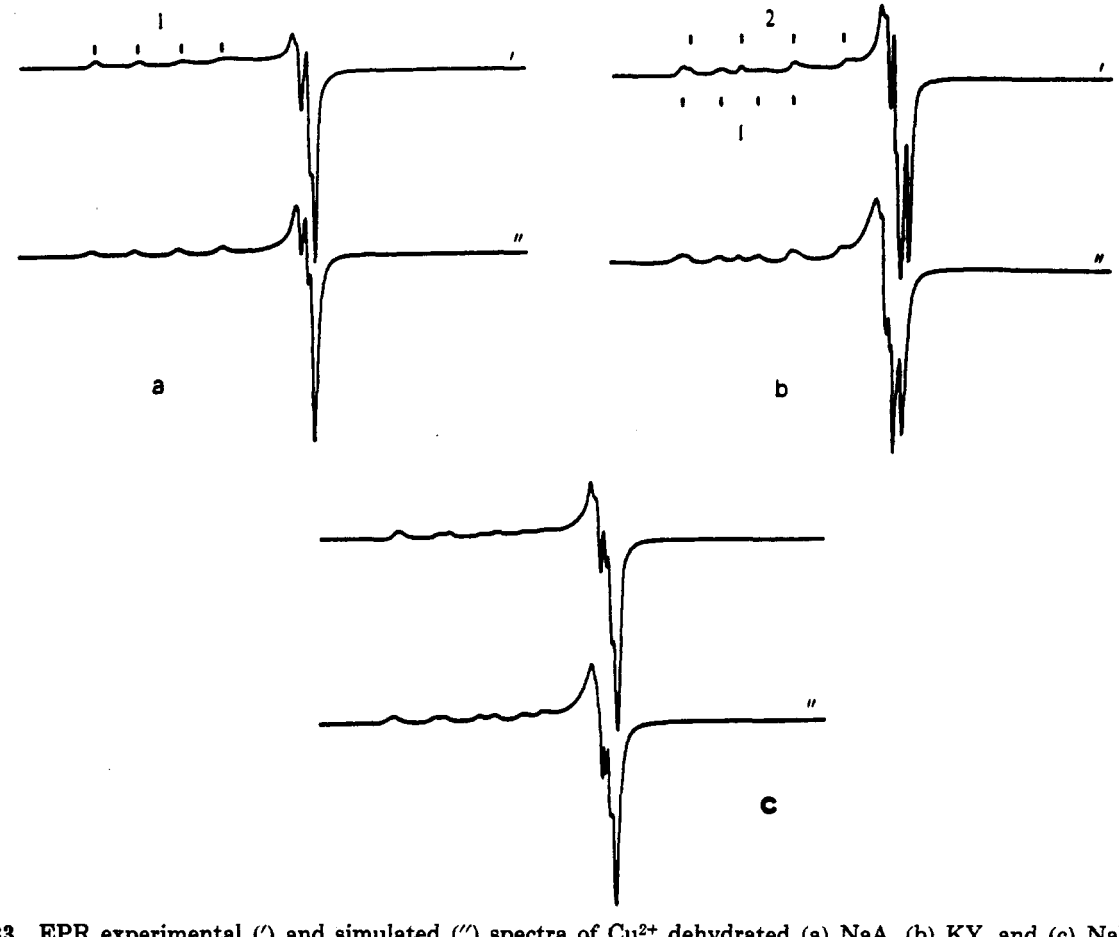

Figure 33. EPR experimental (′) and simulated (″) spectra of Cu^{2+} dehydrated (a) NaA, (b) KY, and (c) NaX zeolites. Reprinted from ref 61. Copyright 1989 Pergamon.

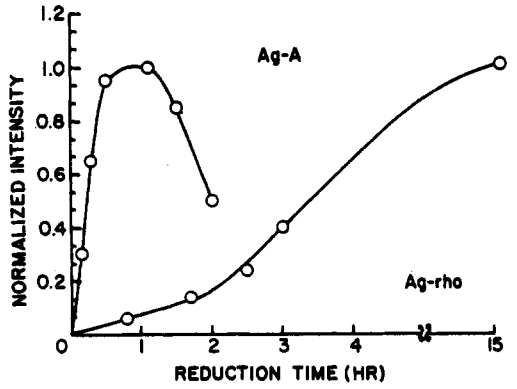

Figure 34. Growth rate of Ag_4A (7 lines) and Ag_7Rho (5 lines) clusters as a function of reduction time in H_2 at room temperature. Reprinted from ref 65. Copyright 1991 American Chemical Society.

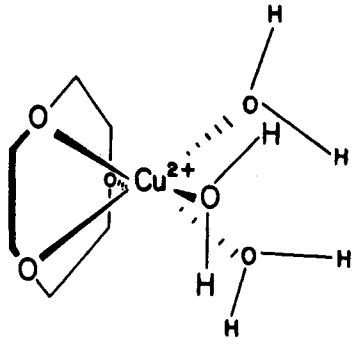

Figure 35. Environment of Cu^{2+} in CuSAPO-5. Reprinted from ref 66. Copyright 1991 American Chemical Society.

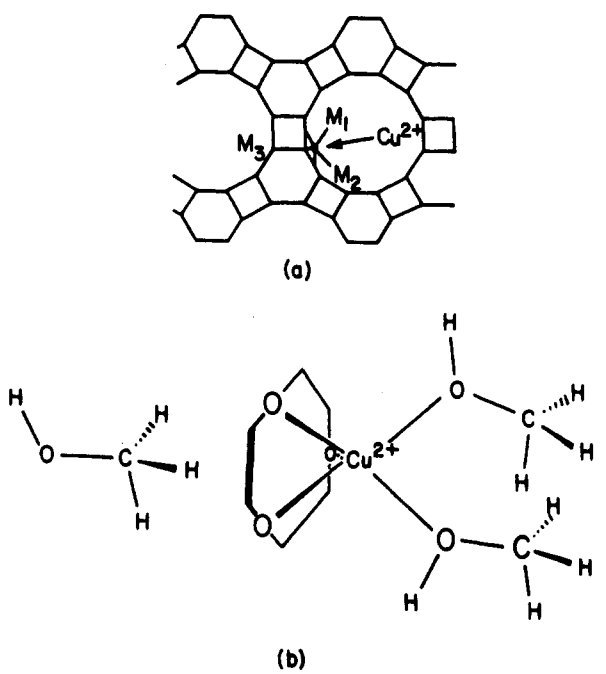

Figure 36. Environment of Cu^{2+} in CuSAPO-5 exposed to CH_3OH: (a) view down 12-ring channel, (b) details of coordination. Reprinted from ref 66. Copyright 1991 American Chemical Society.

state and location of palladium species in pillared montmorillonite[70] and the Cu^{2+} environment of Zr_4 pillared montmorillonite.[71]

A final example of the use of EPR to distinguish different cation sites is the research of Ulla et al.[72] in studies of EuY and EuFeY zeolities. Reduction of Eu-

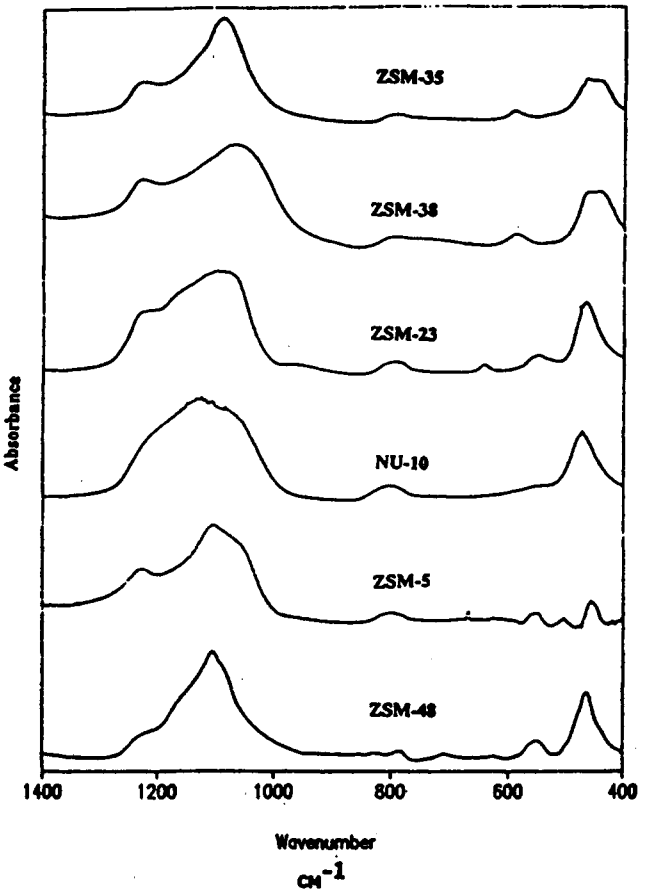

Figure 37. Raman spectra of 5-membered ring zeolite framework structures. Reprinted from ref 73. Copyright 1991 American Chemical Society.

(III) to Eu(II) by either CO or H_2 was monitored by EPR and Mössbauer methods.

B. Optical Methods

1. Raman

Raman methods have been used to study the basic framework structure of a variety of zeolites having similar structures, such as those shown in Figure 37 which all have 5-ring framework structures.[73] Raman methods offer the advantage that in situ studies can be done. The onset of crystallization and tracking of nucleation in mordenite gels[74] as shown in Figure 38 has been correlated to X-ray powder diffraction data for mordenite materials prepared in the presence and absence of organic templates. Nucleation is apparent after 40 h of heat treatment at 190 °C. Similar experiments[74] to those of Figure 38 have suggested that the organic template stabilizes zeolitic precursors during formation of the framework structure.

Raman methods have also been used to probe acidic sites in zeolites by studying dye molecules interacting with Brönsted and Lewis sites in HY materials.[75] The identification of specific oxovanadate ions in layered lithium aluminates[76] and vanadates in layered double hydroxide materials have also recently been probed via Raman techniques.[77]

Raman methods have also been used to probe the formation of dioxygen complexes of transition metal complexes in zeolites,[78] much the same as in the earlier mentioned EPR and ESEM experiments. Evidence

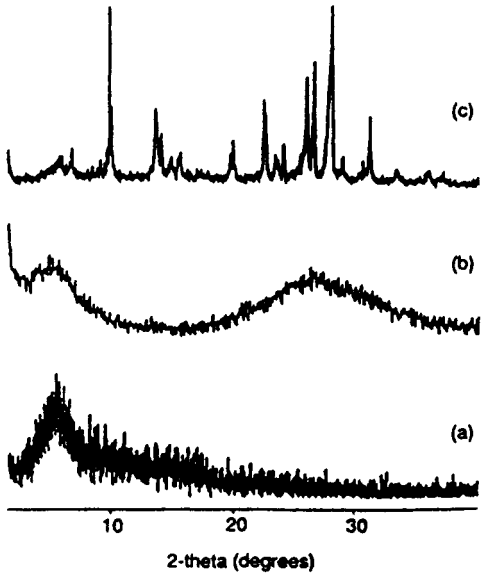

Figure 38. X-ray diffraction patterns of mordenite gels after heating at 190 °C for (a) 4 h, (b) 20 h, and (c) 40 h. Reprinted from ref 74. Copyright 1991 American Chemical Society.

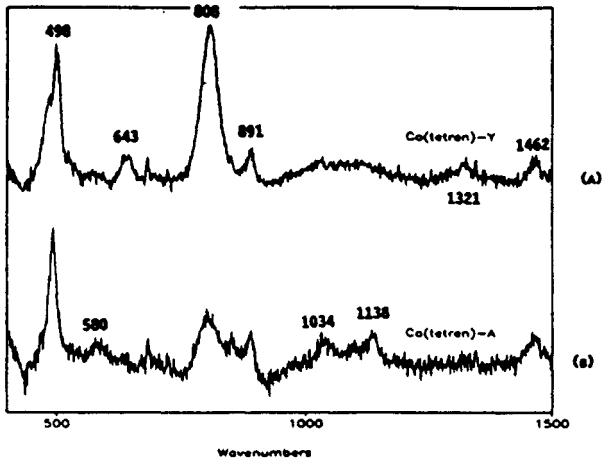

Figure 39. Raman spectra of Co(tetren)-O_2 complex in zeolites (A) Y and (B) A. Reprinted from ref 78. Copyright 1991 American Chemical Society.

for μ-hydroxo complexes of Co(tetren) in Y zeolite by the Raman bands near 498, 643, and 808 cm^{-1} as shown in Figure 39, as well as bands at 580, 1034, and 1138 cm^{-1} for superoxo complexes in zeolite A have been obtained.

In certain cases, various Raman modes such as bond bending and asymmetric and symmetric stretches have been calculated[79] and compared to experimental data. For example, Li, Na, and K sodalite samples were compared by using a nearest-neighbor force model. Agreement between calculated (squares) and experimental (circles) data for such systems is outstanding especially for the bond bending mode as shown in Figure 40. It may be necessary to use more detailed models that incorporate longer range interactions to more accurately predict high-frequency stretching modes.

2. Luminescence

Luminescence methods as applied to zeolites and layered materials have recently been reviewed.[80] Like Raman methods, in situ treatments of gels[81] can be used to study synthesis of zeolitic and layered materials.

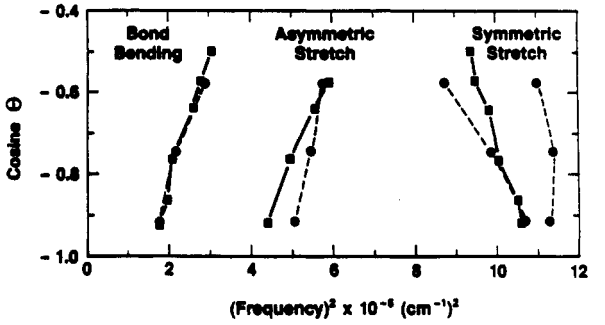

Figure 40. Cosine of inter-tetrahedral angle versus square of mode frequency for Li, Na, and K chloride sodalite. Circles are experimental data; filled squares are results of a nearest-neighbor model calculation. Reprinted from ref 79. Copyright 1988 Materials Research Society.

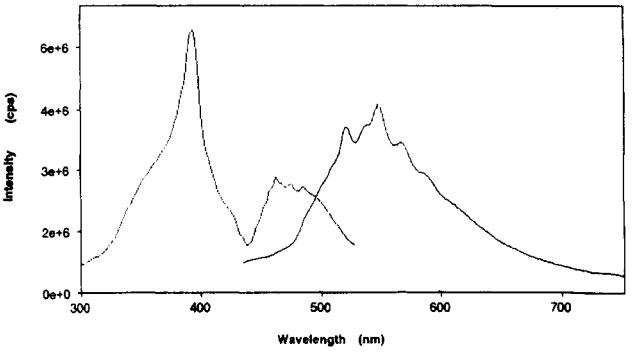

Figure 41. Luminescence excitation (300–500 nm) and emission (500–750 nm) spectra of crystallized B-ZSM-5. Reprinted from ref 56. Copyright 1992 American Chemical Society.

For example, an in situ study[56,81] of the nucleation of B-ZSM-5 crystals via luminescence has shown that tetrahedral B^{3+} can be directly observed with luminescence methods as shown in Figure 41. Absorption occurs at lower wavelengths between 300 and 500 nm whereas emission occurs between 450 and 750 nm. These data have been directly correlated to B NMR data that are given in Figure 29. Emission from Fe^{3+} ions in tetrahedral sites is also well known.[80,81]

Luminescence methods have also been used recently to distinguish Lewis and Brönsted sites in zeolites and alumina.[82] Both phosphorescent and fluorescence transitions were observed in these systems, and emission of pyridine complexes intercalating with Lewis and Brönsted sites exhibited different emission maxima.

Luminescence emission of lanthanide ions in model fluid cracking zeolite catalysts[83] have shown that vanadium poisons interact with lanthanide ions to form lanthanide vanadate species as well as vanadium oxide, V_2O_5. The use of luminescence methods for low-level (parts per million) species is a major advantage of this technique.

Another example is the study of energy transfer in aluminophosphate molecular sieves by Ozin et al.[84] Energy transfer between two nonequivalent Mn(II) centers was proposed for a Förster–Dexter mechanism. The ability to transfer energy in this way is significant, suggesting that long-range (up to 100 Å) interactions may occur.

In montmorillonite and hectorite aqueous suspensions, the fluorescence of methylviologen cations intercalated into the clays[85] was quenched by self-

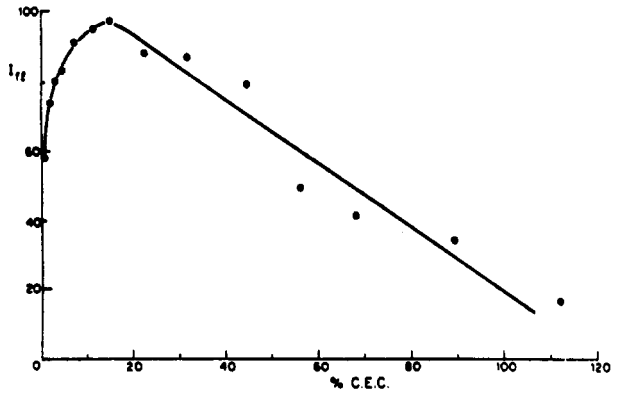

Figure 42. Fluorescence intensity of methylviologen cation in montmorillonite versus cation exchange capacity (CEC) of incorporated methylviologen. Reprinted from ref 85. Copyright 1991 American Chemical Society.

absorption. A decrease in fluorescence intensity of methylviologen as a function of increasing methylviologen exchanged into montmorillonite [greater % CEC (cation exchange capacity)] is shown in Figure 42. These data suggest that only one site is present, and this was further supported by excitation data. Luminescence lifetime data suggest that at least two microenvironments are present for the hectorite system, whereas at least three are found for the montmorillonite methylviologen materials.

3. Infrared Spectroscopy

Ozin and co-workers have compared the use of far-infrared spectroscopy to X-ray diffraction methods and have proposed that a primary use of far-IR is in the determination of various types of cations and their local environments.[86] Amine, phosphine, transition metal, alkali and alkaline earth ions, as well as H^+ can be studied with far-IR.

In situ infrared transmission experiments on ZSM-5 zeolite crystals have recently been used by Nowotny, Lercher, and Kessler[87] to study the rate-determining step for decomposition of organic amine templates. The aluminum concentration in the zeolite crystals controls the dominant type of mechanism for decomposition of template. One mechanism initially involves a Hoffmann elimination followed by a series of β-elimination reactions which proceeds via several steps to form neutral species either in or out of the zeolite. A second mechanism involves initial formation of a cationic tripropylammonium species followed by successive β-eliminations.

Ghosh and Kydd recently reported[88] that FTIR studies of ZSM-5 treated with HF show that dealumination occurs. The severity of HF treatment can yield materials ranging from those with some Lewis acidity to those with no Lewis acidity upon harshest treatments.

4. Diffuse Reflectance Spectroscopy

DRS methods in the ultraviolet–visible (UV–VIS) region of the spectrum have been used by Schoonheydt et al.[89] to study cobalt ions in CoAPO-5 molecular sieves. Figure 43 shows DRS data for CoAPO-5 after treatment in O_2 at 773 K, after treatment with H_2 at 673 K, and after treatment with H_2 at 773 K. These data suggest

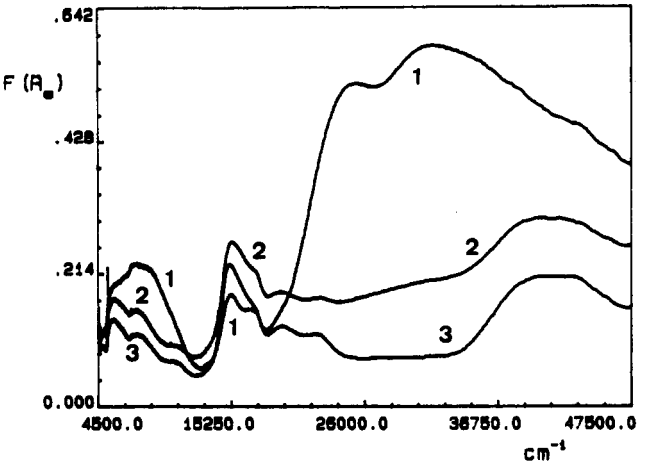

Figure 43. Diffuse reflectance spectra of Co-ALPO-5 after (1) heated in O_2 at 773 K, (2) then reduced in H_2 at 673 K and (3) then reduced at 773 K. Reprinted from ref 89. Copyright 1989 Elsevier.

that tetrahedral Co^{2+} can be reversibly interconverted to Co^{3+} upon oxidation while in the framework of the molecular sieve. This redox behavior may be important in applications of redox catalysis using such materials.

Other examples of the use of DRS to study cations in molecular sieves include Ni^{2+} ions in X and Y zeolites.[90] Ligand field parameters can be obtained from the DRS data and used to distinguish the different environments for nickel before and after thermal treatments in various atmospheres. Schoonheydt and co-workers have demonstrated that the combination of DRS and EPR methods allows for excellent opportunities to study the optical and magnetic environments of ions in molecular sieves, and that these complementary methods provide a good check on each other.

C. Structural

1. X-ray Methods

The structural properties of zeolites, aluminophosphates, and silica clathrates have recently been reviewed by Smith.[91] Structures have been classified by comparing various topologies and geometries into categories such as rings and windows, polyhedral packing, chains, sheets, and nets.

Recent X-ray studies have focused on structural determinations of various zeolites such as the case of zeolite β by Newsam.[92] With a combination of X-ray diffraction, powder neutron diffraction, modeling, and synchrotron neutron diffraction experiments, representations of the two framework structures depicted in Figure 44 were obtained. Zeolite β is believed to be a disordered intergrowth of these two structures.

The importance of modeling for structure determinations has been stressed by the research of Sauer[93] and others. Deem and Newsam[94] have recently derived atomic scale models and T-atom configurations using Monte Carlo calculations. Such methods were used to determine the structure of lithium gallosilicate. An excellent comparison of the [001] projection of calcined lithium gallosilicate to that determined by Monte Carlo methods is shown in Figure 45.

Synchrotron X-ray diffraction methods were recently reviewed by Newsam and Liang.[95] The four major types of powder diffraction configurations as shown in Figure

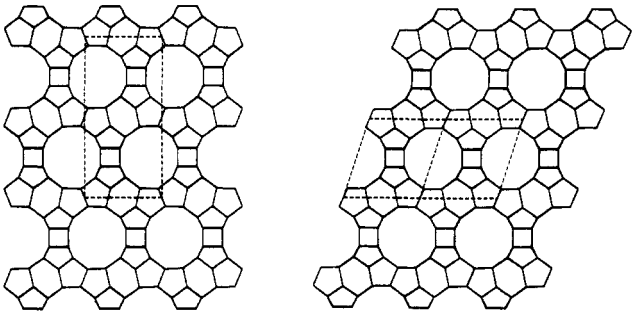

Figure 44. Two framework structures of which zeolite β is a disordered intergrowth. Reprinted from ref 92. Copyright 1990 Kodansha Ltd.

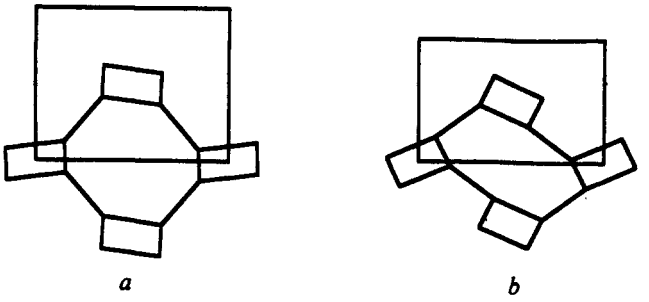

Figure 45. The [001] projections of gallosilicate: (a) compared to distance least-squares (DLS) optimized structure and (b) solved by simulated annealing. Reprinted from ref 94. Copyright 1989 Nature.

46 were discussed. A comparison of synchrotron data to in-house data for a 7-μm zeolite crystal shown in Figure 47 clearly expresses the power of synchrotron experiments.

2. Neutron Methods

Jorgensen et al.[96] have recently reviewed the use of neutron powder diffraction techniques for studies of inorganic materials including light atom systems, magnetic materials, phase transitions, and in situ studies. An example of use of powder neutron diffraction experiments for the determination of binding sites of adsorbates like benzene in dehydrated potas-

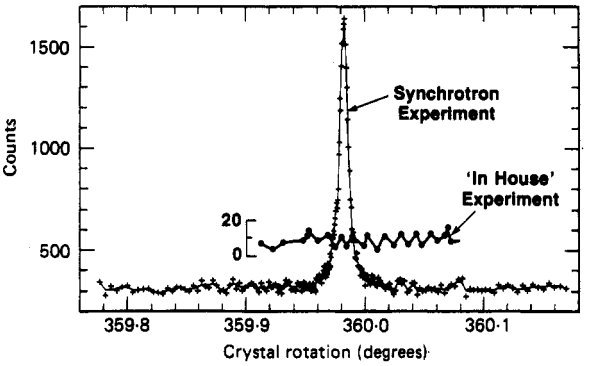

Figure 47. Comparison of synchrotron and in-house diffraction data. Reprinted from ref 95. Copyright 1989 Taylor and Francis.

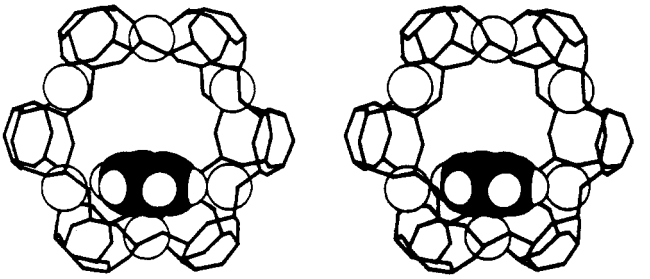

Figure 48. Cross-stereoview of benzene in zeolite KL at 78 K. Reprinted from ref 97. Copyright 1989 American Chemical Society.

sium L zeolite is given in Figure 48 from research of Newsam.[97,98] Neutron diffraction studies of zeolite ρ is flexible, yielding a change in lattice parameter from 15.1 to about 14 Å depending on the type of ion present in the zeolite and specific calcination procedures. Tetrahedrally coordinated Ca^{2+} was observed in this system which may be responsible for this extreme variability. Such variability which may be useful in shape-selective catalysis.

Inelastic and quasinelastic neutron scattering experiments of templates in zeolites and molecular sieves have recently been used by Newsam et al.[101] to study water and hydroxyl groups, hydrocarbon sorbate vi-

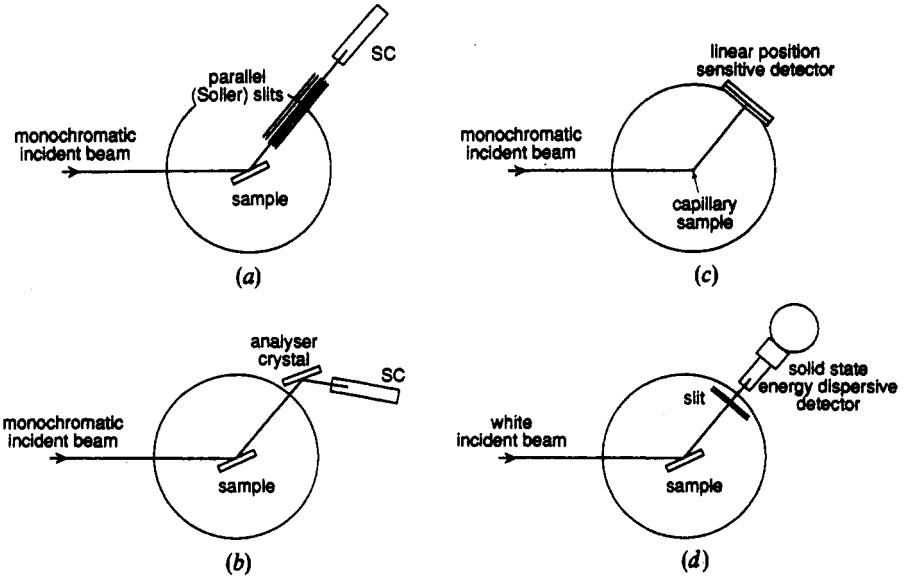

Figure 46. Representations of four sample and detector configurations for synchrotron experiments. Reprinted from ref 95. Copyright 1989 Taylor and Francis.

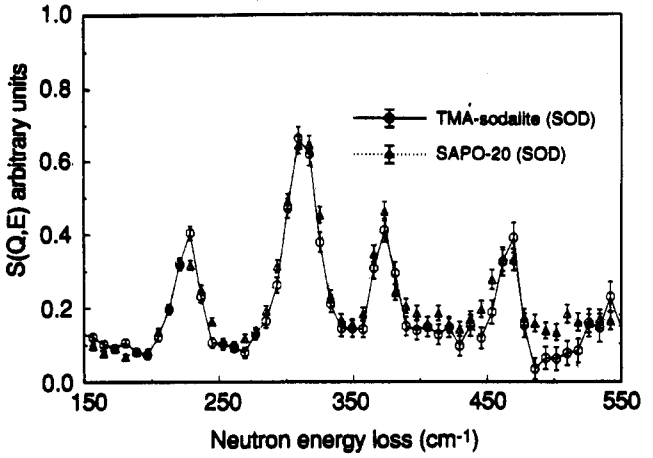

Figure 49. Quasielastic neutron scattering of tetramethylammonium (TMA^+) cations in sodalite (O) compared to a silicoaluminophosphate molecular sieve, SAPO-20, (Δ). Reprinted from ref 101. Copyright 1990 American Chemical Society.

brations, torsional vibrations of cations, and diffusional motion for hydrocarbons in zeolites. A comparison of inelastic neutron scattering (INS) spectra for tetramethylammonium (TMA^+) cations in sodalite and in a silicoaluminophosphate molecular sieve, SAPO-20, shown in Figure 49 suggest that torsional frequencies for TMA^+ are similar in these systems (between 150–550 cm^{-1}). While it appears that INS experiments can be used to obtain information about torsional modes, there seems to be little sensitivity to bending modes.

Small-angle neutron scattering (SANS) experiments of White et al.[102] have been done to probe the mechanism of crystallization of ZSM-5 zeolites. These experiments suggest that templates are incorporated into amorphous embryonic structures which then crystallize via a solid hydrogel transformation. SANS appears to be one of the more useful in situ methods for studying crystallization events in gels.

D. Microscopic Experiments

1. TEM

Transmission electron microscopy (TEM) studies are used to determine morphologies, defect structures, and crystallographic information. Dominguez et al.[103] have recently used TEM methods to investigate pillaring of rectorite with alumina clusters. Electron diffraction methods showed the presence of stacking faults, edges of layers terminating the lattice, and bent stacks. Deformation of alumina pillars and nonuniform distributions of pillars were also apparent from the TEM data.

2. STM, AFM

Scanning tunneling microscopy (STM) experiments have been used to study monolayer assemblies of zirconium phosphonates on mica surfaces by Poireir and co-workers.[104] At a 0.3 monolayer coverage, islands greater than 340 Å were observed that were interconnected.

Atomic force microscopy studies of the surfaces of zeolites have also been investigated by Wiesenhorn et al.[105] and MacDougall and co-workers.[106] Real-time

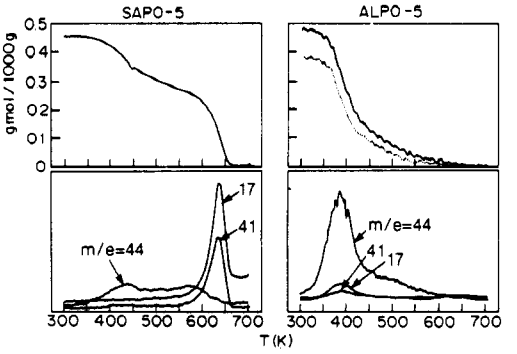

Figure 50. Temperature-programmed desorption (TPD) and thermogravimetric (TGA) data for SAPO-5 and $ALPO_4$-5 after *n*-propylamine sorption; dashed line is for sample calcined with dry O_2. Reprinted from ref 108. Copyright 1991 Academic.

adsorption of tertiary butanol showed production of ordered arrays, whereas adsorption of *tert*-butylammonium cations led to cluster formation.[105] Applications of lithography with such systems were demonstrated. Resolution of different planes of natural zeolites[106] by AFM methods has led to the possibility of monitoring surface reconstruction and ion-exchange events at surfaces of molecular sieves. Since such microscopic methods are relatively new, it would appear that more studies of zeolitic and layered materials will be forthcoming as problems concerning sample treatment, sample handling, and instrumental problems are overcome.

E. Thermal Studies

1. TPD Methods

Temperature-programmed desorption (TPD) methods have primarily been used to study acidity of zeolitic and layered materials. Gorte et al.[107] have proposed the use of isopropylamine as a probe of framework composition and acidity of $ALPO_4$-5 materials. Various metal aluminophosphate materials were also studied. An extension of this research to SAPO-5 done by Biaglow et al.[108] suggested that one Brönsted acid site is generated for every Si substituted into the aluminophosphate material. Mass spectrometry was used to monitor desorption products after *n*-propylamine sorption as shown in Figure 50. It was not possible to tell whether defect sites, aluminophosphate sites, or silicon sites were responsible for enhanced acidity of the SAPO-5 material.

Recent TPD studies of ammonia and pyridine on dealuminated Y zeolites have been carried out by Karge et al.[109] Experiments with ammonia suggested there were at least four types of acid sites, whereas pyridine as an adsorbate yielded only two different acid sites in similar materials. TPD data for ammonia and pyridine are shown in Figures 51 and 52, respectively. Fractional coverages of different sites, activation energies for desorption, and probability functions of activation energies were also determined. Similar studies showing discrepancies between different bases used to titrate acid sites were reported by Karge et al.[110] for dealuminated mordenite zeolites.

Dima and Rees[111] have recently shown that either single or variable heating rates could be used to

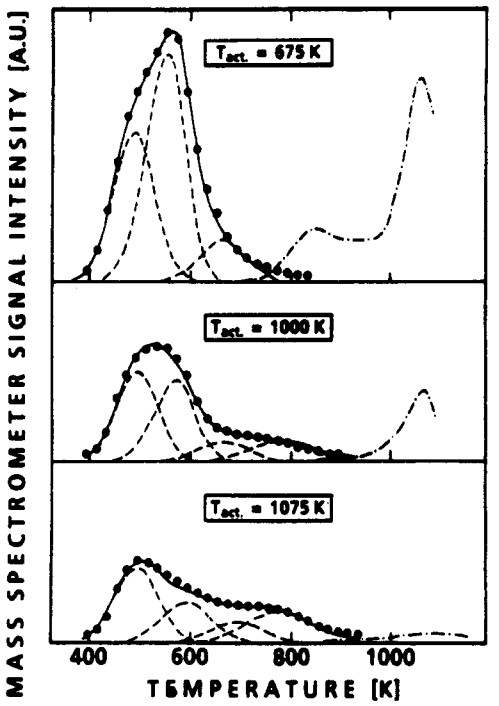

Figure 51. TPD of NH_3 desorbed from dehydroxylated NH_4Y: experimental (—) and theoretical (- - -). Reprinted from ref 109. Copyright 1991 American Chemical Society.

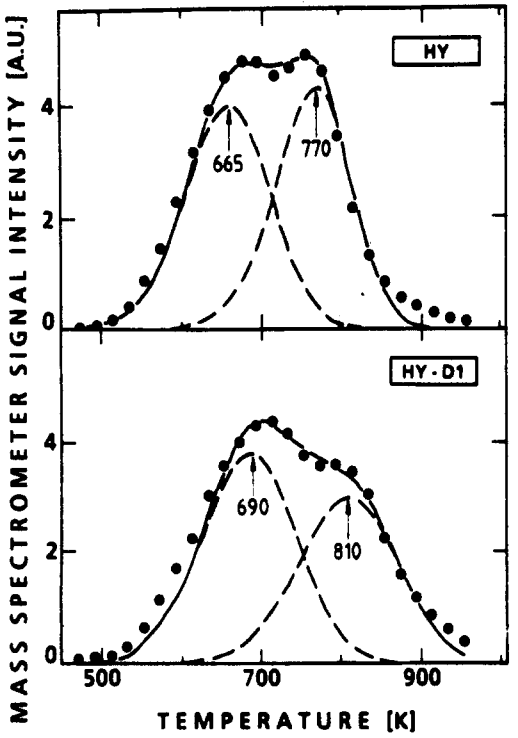

Figure 52. TPD of pyridine desorbed from dehydroxylated NH_4Y: experimental (—) and theoretical (- - -). Reprinted from ref 109. Copyright 1991 American Chemical Society.

determine accurate and reliable activation energies for desorption of ammonia in NaY and HY zeolites during TPD measurements. Assumptions were that first-order kinetics, linear heating rates, and the Arrhenius equation were appropriate.

A combination of TPD and NMR methods was used to study desorption of ammonia from HZSM-5 zeolites by Hunger et al.[112] Activation energy data were comparable to microcalorimetry data, and TPD data

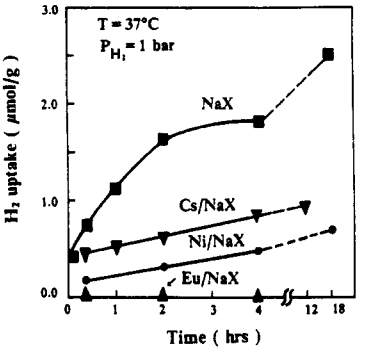

Figure 53. Uptake of H_2 detected by mass spectrometry for various cation-exchanged X zeolites. Reprinted from ref 114. Copyright 1990 Academic.

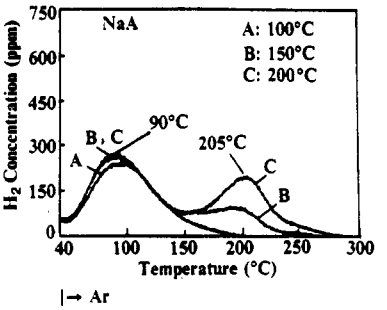

Figure 54. Temperature-programmed desorption (TPD) of H_2 encapsulated in NaA. Temperature for encapsulation of H_2: A = 100 °C; B = 150 °C; C = 200 °C. Reprinted from ref 115. Copyright 1991 Academic.

were simulated using Monte Carlo methods. At least two different Brönsted acid sites were implicated in these studies.

Heats of sorption for aromatics in ZSM-5 zeolites were found to increase with increasing numbers of attached CH_3 groups by Choudhary and co-workers.[113] Correlations of TPD data with Si/Al ratios, dehydration processes, and poisoning studies suggest that Brönsted acid sites are responsible for sorption of aromatics.

2. Transient Kinetics

Transient kinetic studies of gaseous species in zeolites detected by mass spectrometry methods by Efstathiou et al.[114] suggest that molecular hydrogen can be encapsulated in the sodalite cages of NaX zeolite for H_2 pressures of 1 atm. A comparison of encapsulation in various transition metal-exchanged X zeolites is shown in Figure 53. These data imply that sodalite cages are responsible for H_2 encapsulation since in EuNaX, where no encapsulation occurs, the sodalite cages are filled with Eu_4O^{10+} clusters.

Similar results were found by Efstathiou and coworkers[115] for NaA zeolites and transition metal ion-exchanged A zeolites. However, two major desorptions were observed for NaA (Figure 54), CsA, and NiA, with only one observed for EuA. Encapsulation of H_2 in sodalite cages and supercages of these A zeolites (only supercages of EuA) is the major conclusion of these studies. The amounts of H_2 are small but may be important for reactions of zeolites that contain H_2 in any reactant feed. Diffusivities for the different ion-exchanged forms varied due to the accessibility of H_2 into sodalite cages through 6-member windows blocked by certain cations.

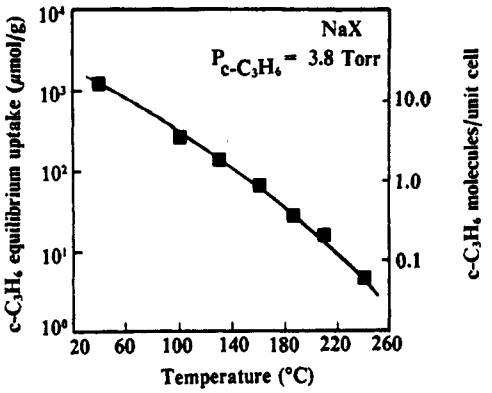

Figure 55. Uptake of c-C_3H_6 by NaX versus temperature. Right y axis represents uptake of c-C_3H_6 molecules per unit cell. Reprinted from ref 116. Copyright 1991 Academic.

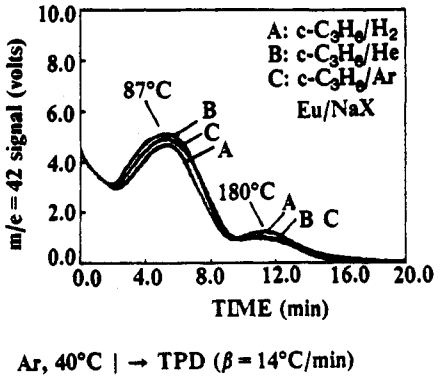

Figure 56. Temperature-programmed desorption (TPD) of c-C_3H_6 in EuNaX: (A) H_2, (B) He, and (C) Ar. Low-temperature peak (87 °C) is c-C_3H_6; high-temperature peak is C_3H_6, as determined by gas chromatography. Reprinted from ref 118. Copyright 1992 Academic.

Transient kinetic studies of cyclopropane in NaX zeolite by Efstathiou et al.,[116] on the other hand, show that cyclopropane is sorbed in the zeolite with activation energies on the order of 11 kcal/mol. A plot of equilibrium uptake of cyclopropane versus temperature is shown in Figure 55 that suggests the gas-phase composition of the pores of the zeolite changes considerably at different reaction temperatures. This result was used to help explain differences in selectivity for hydrogenation, hydrogenolysis, and ring opening reactions over NaX.

Transient sorption of cyclopropane in CsX and NiX zeolites were also reported by Efstathiou and coworkers[117] as well as enthalpies and entropies of sorption for cyclopropane. Enthalpies of sorption are independent of the cation, although entropies of sorption seem to be related to cation content.

Efstathiou et al.[118] also studied sorption of cyclopropane in EuX zeolite. Isomerization to propylene was observed at temperatures as low as 80 °C, and an activation energy of 11 kcal/mol was measured for EuX. Two peaks were observed in the TPD of sorbed cyclopropane as shown in Figure 56. The first peak is due to desorbing cyclopropane, and the second is due to propylene produced during reaction.

The advantages of using transient kinetic methods as outlined above include the detection of surface intermediates, determination of thermodynamic parameters, mechanisms of catalyst deactivation, and the ability to monitor species at low concentrations with mass spectrometry methods at early stages of reaction and sorption.

Table 2. Catalytic Activity of Borosilicate and Gallate Zeolites

catalyst	reactant	reaction	ref
BZSM-5	toluene	disproportionation	121
BZSM-5	1-hexene	isomerization	122
BZSM-5	*n*-heptane; *n*-pentane	cracking; hydroisomerization	123
GaZSM-5	ethane	aromatization	124
GaZSM-5	*n*-butane	aromatization	125
BZSM-5	1-pentene	skeletal isomerization	126

IV. Applications

A. Catalysis

Zeolitic and layered materials are most notably used in catalysis for shape-selective reactions as discussed by Khouw et al.[119] These reactions are primarly acid-catalyzed; however, biocatalytic, electrocatalytic, photocatalytic, and oxidation reactions have also been studied. [See references in Table 1.]

Isomorphously substituted zeolites such as those discussed in the synthesis section have been of intense interest lately due to their potential catalytic activity. Lin et al.[120] have reviewed the use of Fe-ZSM-5 zeolites in methanol conversion and in toluene alkylation. Moderately strong acidity was associated with these Fe-ZSM-5 materials. Isomorphous substitution of boron and gallium in zeolites can lead to a variety of catalytic reactivities as summarized in Table 2.

As observed in Table 2, primarily group IIIA elements have been used for substitutions in ZSM-5, and certain elements appear to enhance catalytic activity of specific reactions. However, Chu et al.[127] have suggested early on that, at least for the BZSM-5 systems, residual Al^{3+} ions are responsible for acid catalysis. Shihabi et al.[128] have shown that incorporation of Al^{3+} from alumina binders leads to incorporation of Al^{3+} in ZSM-5 and production of concomitant acid sites that may be active in catalytic reactions.

At this time, it appears that Ga^{3+} ions are important in aromatization reactions as suggested in the studies of Table 2. Transition metal incorporation via ion-exchange has long been known to influence acidity, and several recent articles have explored the use of specific ions to catalyze certain reactions. For example, Co and Ni zeolites are active for *n*-butene isomerization, oligomerization of olefins occurs via Cd, Zn, Co, and Ni zeolites, and acetylene hydration is activated by late transition metal cations.[129] Further examples include isomerization of olefins with lanthanide ions in zeolites[130] and *n*-hexane cracking and methanol conversion by SAPO-11.[131]

Similar kinds of studies with clays and other layered materials have also been carried out. A unique example is the expansion of clays to produce pillared clays by use of supercritical fluids (CO_2) by Occelli et al.[132] Such pillared clays show higher catalytic cracking activity and selectivity than typical smectite pillared clays. These materials are relatively stable toward steam regeneration treatments and are not severely coked, which are long standing concerns for applications of these materials in cracking catalysis.

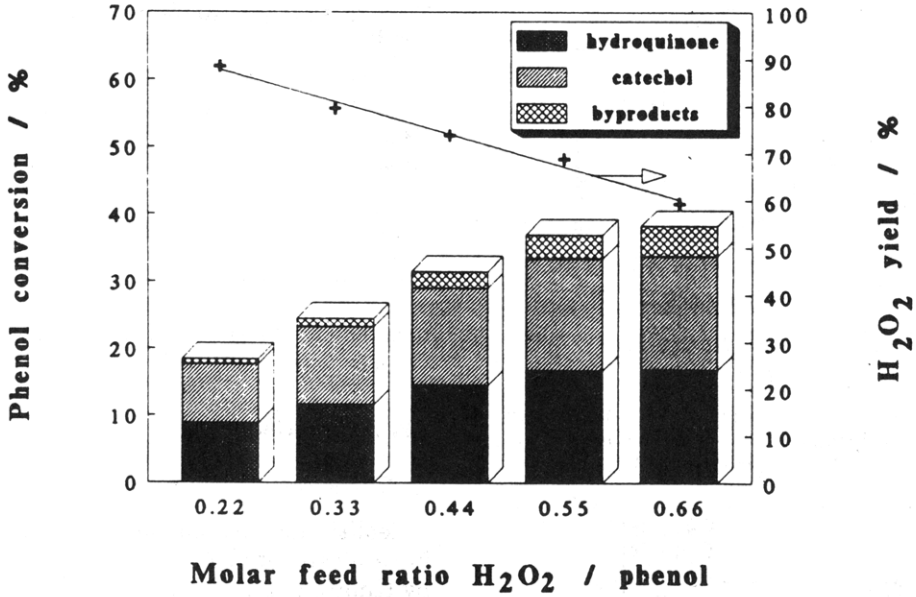

Figure 57. Conversion of hydroxylation of phenol by H_2O_2 versus molar feed ratio of H_2O_2/phenol for titanium pentasil zeolite catalysts. Reprinted from ref 134. Copyright 1998 Elsevier.

Oxidation reactions catalyzed by zeolites have been the recent focus of Jacobs and co-workers.[133-137] Phthalocyanines and porphyrins have been incorporated into large pore zeolites and have been used in catalytic oxidations of olefins and for hydroxylation of aromatics.[133] Ti(IV) substituted in pentasil zeolites has led to interesting oxidations of a variety of substrates such as phenols in the formation of hydroquinone, catechol, and other products as depicted in Figure 57. Restricted transition-state-shape selectivity has been invoked to explain conversions of oxygen-containing substrates like phenol.[134] The concept of zeolite-based enzyme mimics or so-called Zeozymes has also been proposed.[135,136] Oxidation of alkanes by phthalocyanines encaged in zeolites are believed to occur in a regioselective manner on the outermost carbon atoms.[137] Two different types of reaction mechanisms were proposed: free radical reactions over phthalocyanine catalysts and consecutive homolytic reactions over titanium silicate catalysts. Molecular modeling methods[138] have been used to explain the greater shape selectivity of regioselective oxidation of *n*-octane in zeolite Y with respect to other molecular sieves such as VPI-5.

Olefin oxidation over transition metal and encapsulated transition metal complexes has also been of recent interest. Yu and Kevan have studied partial oxidation of propylene to acrolein over Cu^{2+} exchanged X and Y zeolites[139] and mixed Cu^{2+}/alkali–alkaline earth exchanged zeolites.[140] Cuprous ions are believed to be the active sites in both systems. The degree of reoxidation and rehydration is important in regenerating active sites. Manganese salen complexes encapsulated in zeolite Y are active for oxidation of cyclohexene, styrene, stilbene, and octene.[141] Diffusivity is lowered due to encapsulation in the pores of the zeolite leading to lower turnover numbers.

B. Photochemistry

Recent reviews of photochemical studies of zeolitic and layered materials have been published,[142-144] although several new developments are now available. Dyes like methylene blue on hectorite clay surfaces have

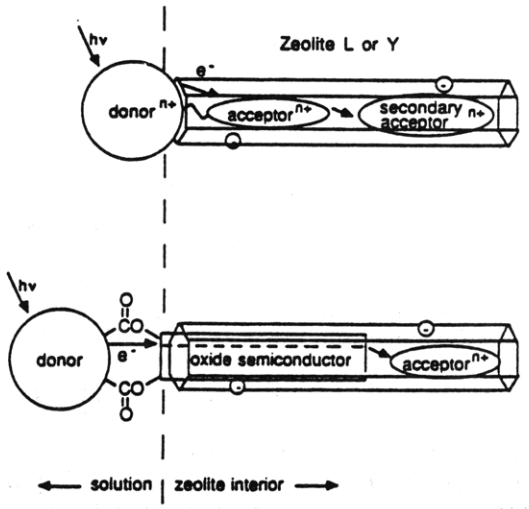

Figure 58. Reaction scheme for light-induced electron-transfer mechanism in zeolites L and Y. Donor at the zeolite solution interface is irradiated and energy is transferred to acceptor molecules (primary or secondary) in the channels of the zeolites. Reprinted from ref 147. Copyright 1990 Plenum.

several forms including monomers, protonated monomers, dimers, and trimers as evidenced by visible spectroscopy.[145] Similar systems have been used to photooxidize tryptophan.[146] Several factors are important in such oxidations, including the degree of Fe^{3+} in the clay which quenches the excited state of the photosensitizer methylene blue, the location of methylene blue, and aggregation of the dye. Clays with a large surface area, especially large external surface areas have been found to be the most active.

The use of zeolites in light-induced electron-transfer mechanisms to mimic artificial photosynthesis has been studied by Krueger et al.[147] A general reaction scheme for the light-induced electron-transfer reactions is shown in Figure 58. Careful design of such a system involves anchoring a donor to the external surface of the zeolite and incorporating acceptor molecules in the channels of the zeolite. Research from Mallouk et al.[144,147] has shown that electron-transfer relays in zeolites can be designed to drive redox reactions.

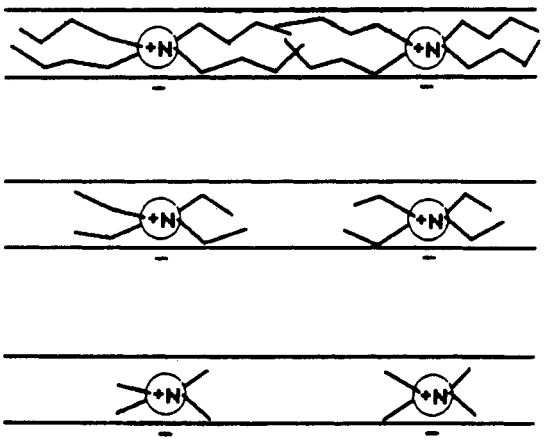

Figure 59. Variation of porosity of hectorite with tetramethyl-, tetraethyl-, and tetra-*n*-butylammonium pillaring agents. Reprinted from ref 151. Copyright 1991 American Chemical Society.

Water-soluble porphyrin complexes have been used to probe the face-to-face aggregation of hectorite particles by Kuykendall and Thomas.[148] Protonation of the porphyrin upon reaction with the clay leads to large shifts in Soret transitions which have also been observed by others.[36] In addition, two major types of interactions of ruthenium bipyridyl complexes on hectorite have been observed.[149] One interaction involves linkage to water molecules at the surface while the other involves direct interaction with the clay surface.

A review of photochemical and photophysical studies of clays has focused on surface configurations as discussed above, organoclay derivatives such as with micelles and surfactants, the production of semiconductors in clays, and photooxidations.[150] It is pointed out that conversions for reactions like water splitting in such systems are small and that further efforts in this area might be warranted.

Pillared clays have also been investigated with photochemical methods[151] and as shown in Figure 59, the orientation of *n*-alkylammonium cation pillaring agents is important for reactivity due to the generation of different microenvironments. The porosity of such systems may be influenced by the nature of the hydrophobicity and chain length of the intercalating amine pillaring agents. Formation of CdS clusters in zeolites and their characterization by photochemical methods have also been reported.[152]

The influence of cation size in rearrangements and disproportionation of alkyl dibenzyl ketones has been studied for different cations in zeolites.[153] Selectivities of products are markedly influenced by both the presence of the zeolite structure and the nature of cations. Heavy atom-induced phosphorescence of naphthalene and polyenes has been investigated in various zeolites,[154] and novel triplet phosphorescence[155] has been observed for the first time for certain polyene configurations.

Norrish type I and II reactions of benzoin[156] and dibenzyl ketones[157] examined by Corbin and co-workers and Ramamurthy et al., respectively, have shown that differences in selectivity are observed for zeolite solvent slurry and dry solid photolyses. Slurry systems are found to be more selective than the dry solid systems.

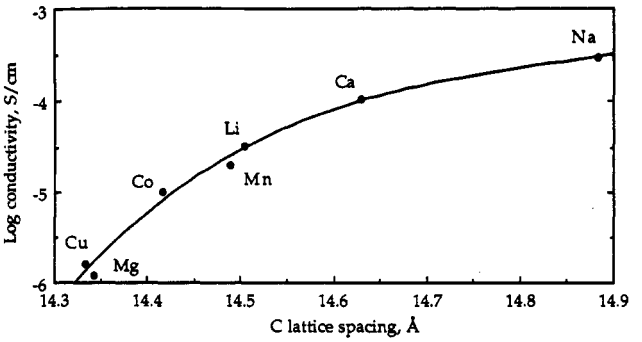

Figure 60. Plot of log conductivity versus c lattice parameter for cation exchanged vermiculites. Reproduced from ref 160 with permission.

C. Electrochemistry

Ionic conductivity of vermiculite has been measured by Whittingham[158] at temperatures ranging from 5 to 90 °C. A hopping mechanism in the interlayer has been proposed for the conductivity which was observed between 5 and 90 °C. The conductivity was enhanced by disassociation (during thermal treatment) of three water molecules from the clay. The major current carriers appear to be cations, not protons.[159] The relationship between conductivity and cation content is manifested in the size of hydrated cations[160] as studied by X-ray methods. A plot of log conductivity versus *c* lattice spacing of ion-exchanged vermiculite samples is shown in Figure 60. Further data on single crystals of vermiculite in the H^+ form suggest that H^+ ions are not the charge carriers,[161] but rather Ca^{2+} cations.

Conductive polymers prepared by intercalation methods have been the focus of several solid-state research groups. Electrochromics, batteries, and other devices are final objectives of much of this research.[162] Conductive polymeric systems designed around porous systems that can be intercalated such as FeOCl are the focus of research by Kanatzidis et al.[163] New materials, phase changes, and mechanisms of conduction are areas of interest.

Self-assembling redox chains of various donors and acceptors bound to zeolite, layered, and pillared clay materials have been studied by Mallouk and co-workers.[164-166] How such species interact at electrode surfaces is depicted in Figure 61 for a zeolite system. The ability to bind specific electron-transfer reagents to external or internal sites is critical in development of such systems.

V. Conclusions

Several areas of current research with zeolitic and layered materials have been discussed above including synthesis, new methods of characterization, and various recent applications. Some of the areas of current interest not touched on in this review include the use of zeolitic and layered materials as nonlinear optics,[167-170] intrazeolite quantum dots and supralattices,[171,172] intrazeolite complexes,[173,174] advanced materials,[175] and as semiconducting materials.[176-182] Materials like layered double hydroxides have also recently been reviewed.[183]

Continuing interest in catalysis includes polymerization of olefins with zeolites and molecular sieves,[184] as well as studies of basic zeolitic materials generated

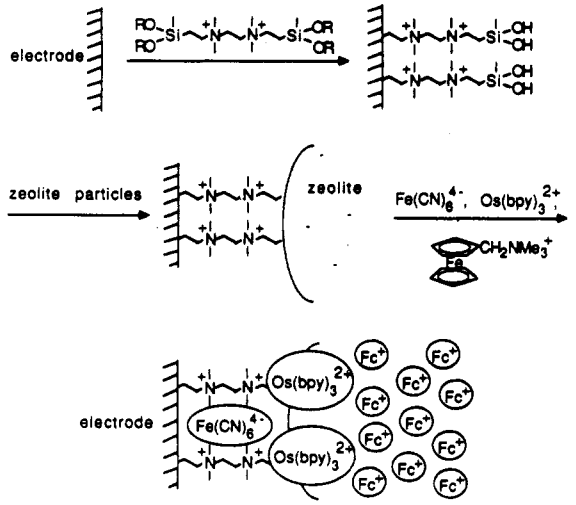

Figure 61. Scheme for self-assembling redox chains at zeolite Y electrodes; Fc^+ = ferrocenyl cation. Reprinted from ref 164. Copyright 1989 American Chemical Society.

by incorporation of alkali ions.[185] Use of organoclay complexes for triphase catalysis is another recent example of new applications of zeolitic and layererd materials.[186] The combination of spectroscopic methods for characterizing materials will continue to be important. Even the more unlikely combinations such as NMR with EPR, such as in the recent study of binding of triethyl phosphate to montmorillonite,[187] have been initiated. Conductivity studies of new porous materials such as germanates[188] and silicogermanates[189] may prove useful for the generation of new conducting materials. Derivatization of phosphonates, for example the preparation of amine and ester functional groups on zirconium phosphonates[190] appears to be an area that will afford several new materials. Sol–gel methods will continue to be important for the preparation of clay and zeolitic materials such as fluorophlogopite,[191] typically prepared by solid-state methods. Specific examples of the use of organoclay materials in molecular recognition includes the work of Lao and co-workers[192] concerning shape-specific separations of CO_2 mixtures. Applications of novel layered materials such as layered niobates intercalated with methylviologen have shown to be useful in light-induced electron-transfer reactions.[193] Undoubtedly there will continue to be a major effort to produce new zeolitic materials in a systematic fashion. The design of intergrowths of cubic and hexagonal phases of faujasites[194] is a specific example. In addition, spectroscopic studies such as MASNMR[195] will continue to be developed for ex and in situ research. Another area that is receiving more and more concern is theoretical modeling such as the material reviewed by Sauer[93] and studies of Newsam et al.[94-98] In addition to such studies, it is now possible to simulate NMR, X-ray diffraction, and electron diffraction data by either using crystallographic parameters for known structures or for hypothetical structures. Applications range from use for synthesis of new materials to predicting spectroscopic data to energy minimization and dynamics studies. It is clear that research in zeolitic and layered materials is healthy and growing and may produce new practical devices for energy-, materials-, and health-related applications.

VI. Acknowledgments

Helpful suggestions from Prof. Mark E. Davis, Dr. Lennox E. Iton, and Prof. C. O. Bennett are greatly appreciated. The author acknowledges support in this area of research from the Department of Energy, Office of Basic Energy Sciences, Division of Chemical Sciences, the National Science Foundation, Engelhard Corp., UNOCAL Corp., Texaco Inc., Mobil, Shell, Phillips Petroleum, Catalytica, ARCO, the American Chemical Society, the Research Corporation, the University of Connecticut, the State of Connecticut Department of Higher Education and Connecticut Innovation, Inc. The author also gratefully acknowledges the technical assistance of Jan Leonard and the availability of preprints and reprints of several researchers for preparation of this review.

References

(1) Pennisi, E. *Sci. News* **1992**, *141*, 228.
(2) Chae, H. K.; Klemperer, W. G.; Payne, D. A.; Suchicital, C. T. A.; Wake, D. R.; Wilson, S. R. In *New Materials for Nonlinear Optical Applications*; Marder, S. R., Sohn, J. E., Stucky, G. D., Eds.; ACS Symposium Series 455; American Chemical Society: Washington, DC, 1991; pp 528–540.
(3) Wilson, S. T.; Lok, B. M.; Messina, C. A.; Cannon, T. R.; Flanigen, E. M. *J. Am. Chem. Soc.* **1982**, *104*, 1146–1147.
(4) Lok, B. M.; Messina, C. A.; Patton, R. L.; Gajek, R. T.; Flanigen, E. M. *J. Am. Chem. Soc.* **1984**, *106*, 6092–6093.
(5) Wilson, S. T.; Flanigen, E. M. In *Zeolite Synthesis*; Occelli, M. L., Robson, H. E., Eds.; ACS Symposium Series 398; American Chemical Society: Washington, DC, 1989; pp 329–345.
(6) Davis, M. E.; Saldarriaga, C.; Montes, C.; Garces, J.; Crowder, C. *Nature* **1988**, *331*, 698–699.
(7) Estermann, M.; McCusker, L. B.; Baerlocher, C.; Merrouche, A.; Kessler, H. *Nature* **1991**, *352*, 320–323.
(8) Gier, T. E.; Stucky, G. D. *Nature* **1991**, *349*, 508–510.
(9) Harrison, W. T. A.; Gier, T. E.; Stucky, G. D. *J. Mater. Chem.* **1991**, *1*, 153–154.
(10) Harrison, W. T. A.; Gier, T. E.; Moran, K. E.; Nicol, J. M.; Eckert, H.; Stucky, G. D. *Chem. Mater.* **1991**, *3*, 27–29.
(11) Nenoff, T. M.; Harrison, W. T. A.; Gier, T. E.; Stucky, G. D. *J. Am. Chem. Soc.* **1991**, *113*, 378–379.
(12) Harrison, W. T. A.; Martin, T. E.; Gier, T. E.; Stucky, G. D. *Chem. Mater.* **1991**, *3*, 27–29.
(13) Annen, J.; Davis, M. E.; Higgins, J. B.; Schlenker, J. L. *J. Chem. Soc., Chem. Commun.* **1991**, 1175–1176.
(14) Lawton, S. L.; Rohrbaugh, W. J. *Science* **1990**, *247*, 1319–1322.
(15) Haushalter, R. C.; Mundi, L. A. *Chem. Mater.* **1992**, *4*, 31–48.
(16) Perez, J. O.; McGuire, N. K.; Clearfield, A. *Catal. Lett.* **1991**, *8*, 145–154.
(17) Duncan, B.; Szostak, R.; Sorby, K.; Ulan, J. G. *Catal. Lett.* **1990**, *7*, 367–376.
(18) Inoue, Y.; Kubokawa, T.; Sato, K. *J. Chem. Soc., Chem. Commun.* **1990**, 1298–1299.
(19) Shen, Y. F.; Zerger, R. P.; DeGuzman, R. D.; Suib, S. L.; O'Young, C. L. *J. Chem. Soc., Chem. Commun.* **1992**, *17*, 1213–1214.
(20) Pinnavaia, T. J. *Science* **1983**, *220*, 4595–4599.
(21) Guan, J.; Min, E.; Yu, Z. U.S. Patent 4,757,040, 1987.
(22) Occelli, M. L. In *Preparation of Catalysts, V*; Poncelot, G., Jacobs, P. A., Delmon, B., Eds.; Elsevier: Amsterdam, 1991; pp 287–299.
(23) Khairy, M.; Tinet, D.; van Damme, H. *J. Chem. Soc., Chem. Commun.* **1990**, 856–857.
(24) Wong, S. T.; Cheng, S. *Inorg. Chem.* **1992**, *31*, 1163–1172.
(25) Drezdon, M. A. *Inorg. Chem.* **1988**, *27*, 4628–4633.
(26) Sterte, J. *Clays Clay Miner.* **1991**, *39*, 167–173.
(27) Chu, C. T. W.; Chang, C. D. *J. Phys. Chem.* **1985**, *89*, 1569–1571.
(28) Bellussi, G.; Millini, R.; Carati, A.; Maddinelli, G.; Gervasini, A. *Zeolites* **1990**, *10*, 642–649.
(29) Vedrine, J. C. In *Guidelines for Mastering the Properties of Molecular Sieves*; Barthomeuf, D., et al., Eds.; Plenum Press: New York, 1990; pp 121–143.
(30) Vedrine, J. C. In *Zeolite Chemistry and Catalysis*; Jacobs, P. A., et al., Eds.; Elsevier Science Publishers: Amsterdam, 1991; pp 25–42.
(31) Dompas, D. H.; Morteir, W. J.; Kenter, O. C. H.; Janssen, M. J. G.; Verduijn, J. P. *J. Catal.* **1991**, *129*, 19–24.
(32) Cichocki, A.; Parasiewicz-Kaczmanska, J.; Michalak, M.; Bus, M. *Zeolites* **1990**, *10*, 577–582.
(33) Dutta, P. K.; Robins, D. *Langmuir* **1991**, *7*, 1048–1050.
(34) Clearfield, A. *Chem. Rev.* **1988**, *88*, 125–148.

(35) Carrado, K. A; Thiyagarajan, P.; Winans, R. E.; Botto, R. E. *Inorg. Chem.* **1991**, *30*, 794–799.
(36) Carrado, K. A.; Winans, R. E. *Chem. Mater.* **1990**, *2*, 328–335.
(37) Mehrotra, V.; Giannelis, E. P. *Solid State Commun.* **1991**, *77*, 155–158.
(38) Iton, L. E.; Trouw, F.; Brun, T. O.; Epperson, J. E.; White, J. W.; Henderson, S. J. *Langmuir* **1992**, *8*, 1045–1048.
(39) Mehrotra, V.; Lombardo, S.; Thompson, M. O.; Giannelis, E. P. *Phys. Rev. B* **1991**, 5786–5790.
(40) Mehrotra, V.; Giannelis, E. P.; Ziolo, R. F.; Rogalskyj *Chem. Mater.* **1992**, *3*, 898–902.
(41) Cao, G.; Lynch, V. M.; Swinnea, J. S.; Mallouk, T. E. *Inorg. Chem.* **1990**, *29*, 2112–2117.
(42) Cao, G.; Mallouk, T. E. *Inorg. Chem.* **1991**, *30*, 1434–1438.
(43) Mallouk, T. E.; Lee, H. *J. Chem. Educ.* **1990**, *67*, 829–834.
(44) Hong, H. G.; Sackett, D. D.; Mallouk, T. E. *Chem. Mater.* **1991**, *3*, 521–527.
(45) Kanatzidis, M. G.; Wu, C. G. *J. Am. Chem. Soc.* **1989**, *111*, 4139–4141.
(46) Wu, C. G.; Marcy, H. O.; DeGroot, D. C.; Kannewurf, C. R.; Kanatzidis, M. G. *Mat. Res. Soc. Sympos. Proc.* **1990**, *173*, 317–322.
(47) Kanatzidis, M. G.; Wu, C. G.; Marcy, H. O.; DeGroot, D. C.; Kannewurf, C. R. *Chem. Mater.* **1990**, *2*, 222–224.
(48) Liu, Y. J.; DeGroot, D. C.; Schlinder, J. L.; Kannewurf, C. R.; Kanatzidis, M. G. *Chem. Mater.* **1991**, *3*, 992–994.
(49) Klinowski, J. *Chem. Rev.* **1991**, *91*, 1459–1479.
(50) Chang, C. D.; Bell, A. T. *Catal. Lett.* **1991**, *8*, 305–316.
(51) Perez, J. O.; Chu, P. J.; Clearfield, A. *J. Phys. Chem.* **1991**, *95*, 9994.
(52) Chu, P. J.; de Mallmann, A.; Lunsford, J. H. *J. Phys. Chem.* **1991**, *95*, 7362–7368.
(53) Laperche, V.; Lambert, J. F.; Prost, R.; Fripiat, J. J. *J. Phys. Chem.* **1990**, *94*, 8821–8831.
(54) de la Caillerie, J. B. D'E.; Fripiat, J. J. *Clays Clay Miner.* **1991**, *3*, 270–280.
(55) Deng, Z.; Lambert, J. F. H.; Fripiat, J. J. *Chem. Mater.* **1989**, *1*, 640–650.
(56) Simon, M. W.; Nam, S. S.; Xu, W. Q.; Suib, S. L.; Edwards, J. C.; O'Young, C. L. *J. Phys. Chem.* **1992**, *96*, 6381–6388.
(57) Lazo, N. D.; Richardson, B. R.; Schettler, P. D.; White, J. L.; Munson, E. J.; Haw, J. F. *J. Phys. Chem.* **1991**, *95*, 9420–9425.
(58) Hunger, M.; Freude, D.; Pfeifer, H. *J. Chem. Soc., Faraday Trans.* **1991**, *87*, 657–662.
(59) van Eck, E. R. H.; Janssen, R.; Maas, W. E. J. R.; Veeman, W. S. *Chem. Phys. Lett.* **1990**, *174*, 428–432.
(60) Park, J. W.; Chon, H. *J. Catal.* **1992**, *133*, 159–169.
(61) Schoonheydt, R. A. *J. Phys. Chem. Solids* **1989**, *50*, 523–539.
(62) Schoonheydt, R. A.; Vaesen, I.; Leeman, H. *J. Phys. Chem.* **1989**, *93*, 1515–1521.
(63) De Tavernier, S.; Schoonheydt, R. A. *Zeolites* **1991**, *11*, 155–163.
(64) Janssens, C.; Grobet, P. J.; Schoonheydt, R. A.; Jansen, J. C. *Zeolites* **1991**, *11*, 184–191.
(65) Xu, B.; Kevan, L. *J. Phys. Chem.* **1991**, *95*, 1147–1151.
(66) Chen, X.; Kevan, L. *J. Am. Chem. Soc.* **1991**, *113*, 2861–2865.
(67) Brouet, G.; Chen, X.; Kevan, L. *J. Phys. Chem.* **1991**, *95*, 4928–4929.
(68) Lei, G. D.; Kevan, L. *J. Phys. Chem.* **1991**, *95*, 4506–4514.
(69) Brown, D. R.; Luca, V.; Kevan, L. *J. Chem. Soc., Faraday Trans.* **1991**, *87*, 2749–2754.
(70) Luca, V.; Kukkadapu, R.; Kevan, L. *J. Chem. Soc., Faraday Trans.* **1991**, *87*, 3083–3089.
(71) Kukkadapu, R.; Kevan, L. *J. Chem. Soc., Faraday Trans.* **1990**, *86*, 691–696.
(72) Ulla, M. A.; Aparicio, L. A.; Balse, V. R.; Dumesic, J. A.; Millman, W. S. *J. Catal.* **1990**, *123*, 195–205.
(73) Dutta, P. K.; Rao, K. M.; Park, J. Y. *J. Phys. Chem.* **1991**, *95*, 6654–6656.
(74) Twu, J.; Dutta, P. K.; Kresge, C. T. *J. Phys. Chem.* **1991**, *95*, 5267–5271.
(75) Place, R. D.; Dutta, P. K. *Anal. Chem.* **1991**, *63*, 348–351.
(76) Twu, J.; Dutta, P. K. *J. Phys. Chem.* **1989**, *93*, 7863–7868.
(77) Twu, J.; Dutta, P. K. *J. Catal.* **1990**, *124*, 503–510.
(78) Dutta, P. K.; Bowers, C. *Langmuir* **1991**, *7*, 937–940.
(79) Buckley, R. G.; Deckman, H. W.; Newsam, J. M.; McHenry, J. A.; Persans, P. D.; Witzke, H. In *Microstructure and Properties of Catalysts*; Treacy, M. M. J., Thomas, J. M., White, J. M., Eds.; Mater Res. Soc. Sympos. Proc. 111; MRS: Pittsburgh, PA 1988; pp 141–146.
(80) Suib, S. L. In *Focus on Photochemistry*; CRC Press: Boca Raton, FL, 1991; pp 1–40.
(81) Pott, G. T.; Stork, W. H. J. *Catal. Rev.-Sci. Eng.* **1975**, *12*, 163–199.
(82) Szedlacsek, P.; Suib, S. L.; Deeba, M.; Koermer, G. S. *J. Chem. Soc., Chem. Commun.* **1990**, *21*, 1531–1532.
(83) Kurihara, L. K.; Occelli, M. L.; Suib, S. L. in ACS Symp. Ser. **1991**, *452*, 224–231.
(84) Ozin, G. A.; Kuperman, A.; Wiggenhauser, H. *Polym. Preprints* **1989**, *30*, 552–553.
(85) Villemure, G.; Detellier, C.; Szabo, A. G. *Langmuir* **1991**, *7*, 1215–1221.
(86) Ozin, G. A.; Baker, M. D.; Godber, J.; Gil, C. J. *J. Phys. Chem.* **1989**, *93*, 2899–2908.
(87) Nowotny, M.; Lercher, J. A.; Kessler, H. *Zeolites* **1991**, *11*, 454–459.
(88) Ghosh, A. K.; Kydd, R. A. *Zeolites* **1990**, *10*, 766–773.
(89) Schoonheydt, R. A.; de Vos, R.; Pelgrims, J.; Leeman, H. In *Zeolites: Facts, Figures, Future*; Elsevier Science Publishers: Amsterdam, 1989; pp 559–568.
(90) Schoonheydt, R. A.; Roodhooft, D.; Leeman, H. *Zeolites* **1987**, *7*, 412–417.
(91) Smith, J. V. *Chem. Rev.* **1988**, *88*, 149–182.
(92) Newsam, J. M. *Chemistry of Microporous Materials*; Kodansha Ltd.: Tokyo, 1990; pp 133–140.
(93) Sauer, J. *Chem. Rev.* **1989**, *89*, 199–255.
(94) Deem, M. W.; Newsam, J. M. *Nature* **1989**, *342*, 260–262.
(95) Newsam, J. M.; Liang, K. S. *Int. Rev. Phys. Chem.* **1989**, *8*, 289–338.
(96) Jorgensen, J. D.; Newsam, J. M. *MRS Bull.* **1990**, *XV*, 49–55.
(97) Newsam, J. M. *J. Phys. Chem.* **1989**, *93*, 7689–7694.
(98) Newsam, J. M. *Mater. Sci. Forum* **1988**, *27/28*, 385–396.
(99) Corbin, D. R.; Abrams, L.; Jones, G. A.; Eddy, M. M.; Harrison, W. T. A.; Stucky, G. D.; Cox, D. E. *J. Am. Chem. Soc.* **1990**, *112*, 4821–4830.
(100) Corbin, D. R.; Abrams, L.; Jones, G. A.; Eddy, M. M.; Stucky, G. D.; Cox, D. E. *J. Chem. Soc., Chem. Commun.* **1989**, 42–43.
(101) Newsam, J. M.; Brun, T. O.; Trouw, F.; Iton, L. E.; Curtiss, L. A. In *Novel Materials in Heterogeneous Catalysis*; Baker, R. T. K., Murrell, L. L., Eds.; ACS Symposium Series 437; American Chemical Society: Washington, DC, 1990; pp 25–37.
(102) White, J. W.; Henderson, S. J.; Iton, L. E.; Trouw, F.; Brun, T. O.; Epperson, J. E. *Langmuir*, submitted for publication.
(103) Dominguez, J. M.; Occelli, M. L. *Synthesis of Microporous Materials, Expanded Clays and Other Microporous Solids, 2*; Ocelli, M. L., Robson, H. E., Eds.; Van Nostrand Reinhold: New York, 1992; pp 81–107. *Clay Synthesis*; ACS Sympos. Series; American Chemical Society: Washington, DC, 1992; in press.
(104) Poirier, G. E.; Lee, H.; Hance, B. K.; White, J. M.; Mallouk, T. E. *Langmuir*, submitted for publication.
(105) Weisenhorn, A. L.; MacDougall, J. E.; Gould, S. A. C.; Cox, S. D.; Wise, W. S.; Massie, J.; Maivald, P.; Elings, V. B.; Stucky, G. D.; Hansma, P. K. *Science* **1990**, *247*, 1330–1333.
(106) MacDougall, J. E.; Cox, S. D.; Stucky, G. D.; Weisenhorn, A. L.; Hansma, P. K.; Wise, W. S. *Zeolites* **1991**, *11*, 429–433.
(107) Gorte, R. J.; Kokotailo, G. T.; Biaglow, A. I.; Parrillo, D.; Pereira, C. In *Zeolite Chemistry and Catalysis*; Jacobs, P. A., Jaeger, N. I.; Kubelkova, L., Wichterlova, B., Eds.; Elsevier: Amsterdam, 1991; pp 181–187.
(108) Biaglow, A. I.; Adamao, A. T.; Kokotailo, G. T.; Gorte, R. J. *J. Catal.* **1991**, *131*, 252–259.
(109) Karge, H. G.; Dondur, V.; Weitkamp, J. *J. Phys. Chem.* **1991**, *95*, 283–288.
(110) Karge, H. G.; Dondur, V. *J. Phys. Chem.* **1990**, *94*, 765–772.
(111) Dima, E.; Rees, L. V. C. *Zeolites* **1990**, *10*, 8–15.
(112) Hunger, B.; Hoffman, J.; Heitzsch, O.; Hunger, M. *J. Thermal Anal.* **1990**, *36*, 1379–1391.
(113) Choudhary, V. R.; Srinivasan, K. R.; Singh, A. P. *Zeolites* **1990**, *10*, 16–20.
(114) Efstathiou, A. M.; Suib, S. L.; Bennett, C. O. *J. Catal.* **1990**, *123*, 456–462.
(115) Efstathiou, A. M.; Borgstedt, E. V. R.; Suib, S. L.; Bennett, C. O. *J.* 4Catal. **1991**, *135*, 135–146.
(116) Efstathiou, A. M.; Suib, S. L.; Bennett, C. O. *J. Catal.* **1991**, *131*, 94–103.
(117) Efstathiou, A. M.; Suib, S. L.; Bennett, C. O. *J. Catal.* **1992**, *135*, 236–245.
(118) Efstathiou, A. M.; Suib, S. L.; Bennett, C. O. *J. Catal.* **1992**, *135*, 223–235.
(119) Khouw, C. B.; Davis, M. E. In *Selectivity in Catalysis*; Davis, M. E., Suib, S. L., Eds.; ACS Symposium Series; American Chemical Society: Washington, DC, in press.
(120) Lin, D. H.; Coudurier, G.; Vedrine, J. C. in *Zeolites: Facts, Figures, Future*; Jacobs, P. A., van Santen, R. A., Eds.; Elsevier Science Publishers: Amsterdam, 1989; pp 1431–1448.
(121) Sayed, M. B.; Auroux, A.; Vedrine, J. C. *J. Catal.* **1989**, *116*, 1–10.
(122) Cornaro, U.; Wojciechowski, B. W. *J. Catal.* **1989**, *120*, 182–191.
(123) Wendlandt, K. P.; Unger, B.; Becker, K. *Appl. Catal.* **1990**, *66*, 111–122.
(124) Schulz, P.; Baerns, M. *Appl. Catal.* **1991**, *78*, 15–29.
(125) Van Mao, R. L.; Yao, J. *Appl. Catal.* **1991**, *79*, 77–87.
(126) Bianchi, D.; Simon, M. W.; Nam, S. S.; Xu, W. Q.; Suib, S. L.; O'Young, C. L. *J. Am. Chem. Soc.*, submitted for publication.
(127) Chu, C. T. W.; Kuehl, G. H.; Lago, R. M.; Chang, C. D. *J. Catal.* **1985**, *93*, 451–458.
(128) Shihabi, D. S.; Garwood, W. E.; Chu, P.; Miale, J. N.; Lago, R. M.; Chu, C. T. W.; Chang, C. D. *J. Catal.* **1985**, *93*, 471–474.
(129) Kallo, D.; Onyestyak, G. *J. Mol. Catal.* **1990**, *62*, 307–320.
(130) Baba, T.; Koide, R.; Ono, Y. *J. Chem. Soc., Chem. Commun.* **1991**, 691–692.

(131) Khouzami, R.; Coudurier, G.; Mentzen, B. F.; Vedrine, J. C. In *Innovation in Zeolite Materials Science*; Grobet, P. J., et al., Eds.; Elsevier Science Publishers: Amsterdam, 1991; pp 355–363.
(132) Occelli, M. L.; Takahama, K.; Yokoyama, M.; Hirao, S. *Synthesis of Microporous Materials, Expanded Clays and Other Microporous Solids, 2*; Occelli, M. L., Robson, H. E., Eds.; Van Nostrand Reinhold: New York, 1992; pp 57–80.
(133) Huybrechts, D. R. C.; Pareton, R. F.; Jacobs, P. A. In *Chemistry of Microporous Crystals*; Delmon, B., Yates, J. T., Eds.; Elsevier Science Publishers: Amsterdam, 1991; pp 225–254.
(134) Parton, R. F.; Jacobs, J. M.; Van Ooteghem, H.; Jacobs, P. A. In *Zeolites as Catalysts, Sorbents and Detergent Builders*; Karge, H. G., Weitkamp, J., Eds.; Elsevier Science Publishers: Amsterdam, 1989; pp 211–222.
(135) Parton, R. F.; Jacobs, J. M.; Huybrechts, D. R.; Jacobs, P. A. In *Zeolites as Catalysts, Sorbents and Detergent Builders*; Karge, H. G., Weitkamp, J., Eds.; Elsevier Science Publishers: Amsterdam, 1989; pp 763–792.
(136) Parton, R. F.; De Vos, D.; Jacobs, P. A. Proc. NATO Workshop, Portugal; Elsevier: Amsterdam, in press.
(137) Parton, R. F.; Huybrechts, D. R. C.; Buskens, P.; Jacobs, P. A. *Stud. Surf. Sci. Catal.* **1990**, 20–23.
(138) Parton, R. F.; Uytterhoeven, L.; Jacobs, P. A. *Stud. Surf. Sci. Catal.* **1991**, *59*, 395–403.
(139) Yu, J.; Kevan, L. *J. Phys. Chem.* **1991**, *95*, 6648–6653.
(140) Yu, J.; Kevan, L. *J. Phys. Chem.* **1991**, *95*, 3262–3271.
(141) Bowers, C.; Dutta, P. K. *J. Catal.* **1990**, *122*, 271–279.
(142) Turro, N. J. *Pure Appl. Chem.* **1986**, *58*, 1219–1224.
(143) Ramamurthy, V. In *Inclusion Phenomena and Molecular Recognition*; Atwood, J., Ed.; Plenum Press: New York, 1990; pp 351–363.
(144) Krueger, J. S.; Mallouk, T. E. In *Kinetics and Catalysis in Microheterogeneous Systems*; Gratzel, M., Kalyanasundaram, K., Eds.; Marcel Dekker: New York, 1991; pp 461–490.
(145) Cenens, J.; Schoonheydt, R. A. *Clays Clay Miner.* **1988**, *36*, 214–224.
(146) Cenens, J.; Schoonheydt, R. A. *Clay Miner.* **1988**, *23*, 205–212.
(147) Krueger, J. S.; Lai, C.; Li, Z.; Mayer, J. E.; Mallouk, T. E. In *Inclusion Phenomena and Molecular Recognition*; Atwood, J., Ed.; Plenum Press: New York, 1990; pp 365–378.
(148) Kuykendall, V. G.; Thomas, J. K. *Langmuir* **1990**, *6*, 1350–1356.
(149) Kuykendall, V. G.; Thomas, J. K. *J. Phys. Chem.* **1990**, *94*, 4224–4230.
(150) Thomas, J. K. *Acc. Chem. Res.* **1988**, *21*, 275–280.
(151) Kuykendall, V. G.; Thomas, J. K. *Langmuir* **1990**, *6*, 1346–1350.
(152) Liu, X.; Thomas, J. K. *Langmuir* **1989**, *5*, 58–66.
(153) Ramamurthy, V.; Corbin, D. R.; Eaton, D. F. *Tetrahedron Lett.* **1989**, *30*, 5833–5836.
(154) Caspar, J. V.; Ramamurthy, V.; Corbin, D. R. *Coord. Chem. Rev.* **1990**, *97*, 225–236.
(155) Ramamurthy, V.; Caspar, J. V.; Corbin, D. R.; Schlyer, B. D.; Maki, A. H. *J. Phys. Chem.* **1990**, *94*, 3391–3393.
(156) Corbin, D. R.; Eaton, D. F.; Ramamurthy, V. *J. Am. Chem. Soc.* **1988**, *110*, 4848–4849.
(157) Ramamurthy, V.; Corbin, D. R.; Turro, N. J.; Zhang, Z.; Garcia-Garibay, M. A. *J. Org. Chem.* **1991**, *56*, 255–261.
(158) Whittingham, M. S. *Sol. State Ionics* **1989**, *32/33*, 344–349.
(159) Maraqah, H.; Li, J.; Whittingham, M. S. *MRS Symp. Proc. 210*; MRS: Pittsburgh, PA, 1991; pp 351–357.
(160) Li, J.; Whittingham, M. S. *Mat. Res. Bull.* **1991**, *26*, 849–856.
(161) Maraqah, H.; Li, J.; Whittingham, M. S. *J. Electrochem. Soc.* **1991**, *138*, L61–L63.
(162) Kanatzidis, M. G. *Chem. Eng. News* **1990**, *68* (Dec 3), 36–54.
(163) Kanatzidis, M. G.; Wu, C. G.; Marcy, H. O.; DeGroot, D. C.; Kannewurf, C. R.; Kostikas, A.; Papaefthymiou, V. *Adv. Mat.* **1990**, *2*, 364–366.
(164) Li, Z.; Lai, C.; Mallouk, T. E. *Inorg. Chem.* **1989**, *28*, 178–182.
(165) Rong, D.; Kim, Y. I.; Mallouk, T. E. *Inorg. Chem.* **1990**, *29*, 1531–1535.
(166) Rong, D.; Hong, H. G.; Kim, Y. I.; Krueger, J. S.; Mayer, J. E.; Mallouk, T. E. *Coord. Chem. Rev.* **1990**, *97*, 237–248.
(167) Cooper, S.; Dutta, P. K. *J. Phys. Chem.* **1990**, *94*, 114–118.
(168) Cox, S. D.; Gier, T. E.; Stucky, G. D. *Sol. State Ionics* **1989**, *32/33*, 514–520.
(169) Eddy, M. M.; Gier, T. E.; Keder, N. L.; Stucky, G. D.; Cox, D. E.; Bierlein, J. D.; Jones, G. *Inorg. Chem.* **1988**, *27*, 1856–1858.
(170) Nicol, J. M.; Udovic, T. J.; Bush, J. J.; Cox, S. D.; Stucky, G. D. *MRS Proc. 166*; MRS: Pittsburgh, PA, 1990; pp 193–198.
(171) Ozin, G. A.; Kirkby, S.; Meszaros, M.; Ozkar, S.; Stein, A.; Stucky, G. D. In *Materials for Nonlinear Optics*; Marder, S. R., Sohn, J. E., Stucky, G. D., Eds.; ACS Symposium Series 455; American Chemical Society: Washington, DC, 1990; pp 554–581.
(172) Stein, A.; Meszaros, M.; Macdonald, P. M.; Ozin, G. A.; Stucky, G. D. *Adv. Mater.* **1991**, *6*, 306–309.
(173) Ozin, G. A.; Gil, C. *Chem. Rev.* **1989**, *89*, 1749–1764.
(174) Ozin, G. A.; Godber, J. *J. Phys. Chem.* **1989**, *93*, 878–893.
(175) Ozin, G. A.; Kuperman, A.; Stein, A. *Angew. Chem.* **1989**, *101*, 373–390.
(176) Parise, J. B.; MacDougall, J. E.; Herron, N.; Farlee, R.; Sleight, A. W.; Wang, Y.; Bein, T.; Moller, K.; Moroney, L. M. *Inorg. Chem.* **1988**, *27*, 221–228.
(177) Moller, K.; Bein, T.; Herron, N.; Mahler, W.; Wang, Y. *Inorg. Chem.* **1989**, *28*, 2914–2919.
(178) Wang, Y.; Herron, N. *J. Phys. Chem.* **1988**, *92*, 4988–4994.
(179) MacDougall, J. E.; Eckert, H.; Stucky, G. D.; Herron, N.; Wang, Y.; Moller, K.; Bein, T.; Cox, D. *J. Am. Chem. Soc.* **1989**, *111*, 8006–8007.
(180) Herron, N.; Wang, Y.; Eddy, M. M.; Stucky, G. D.; Cox, D. E.; Moller, K.; Bein, T. *J. Am. Chem. Soc.* **1989**, *111*, 530–540.
(181) Moller, K.; Eddy, M. M.; Stucky, G. D.; Herron, N.; Bein, T. *J. Am. Chem. Soc.* **1989**, *111*, 2564–2571.
(182) Stein, A.; Macdonald, P. M.; Ozin, G. A.; Stucky, G. D. *J. Phys. Chem.* **1990**, *94*, 6943–6948.
(183) Cavani, F.; Trifiro, F.; Vaccari, A. *Catal. Today* **1991**, *11*, 173–301.
(184) Cox, S. D.; Stucky, G. D. *J. Phys. Chem.* **1991**, *95*, 710–720.
(185) Barthomeuf, D.; Coudurier, G.; Vedrine, J. C. *Mat. Chem. Phys.* **1988**, *18*, 553–575.
(186) Lin, C. L.; Pinnavaia, T. J. *Chem. Mater.* **1991**, *3*, 213–215.
(187) O'Brien, P.; Williamson, C. J.; Groombridge, C. J. *Chem. Mater.* **1991**, *3*, 276–280.
(188) Feng, S.; Tsai, M.; Greenblatt, M. *Chem. Mater.* **1992**, *4*, 388–393.
(189) Feng, S.; Tsai, M.; Szu, S. P.; Greenblatt, M. *Chem. Mater.* **1992**, *4*, 468–472.
(190) Burwell, D. A.; Thompson, M. E. *Chem. Mater.* **1991**, *3*, 730–737.
(191) Duldulao, F. D.; Burlitch, J. M. *Chem. Mater.* **1991**, *3*, 772–775.
(192) Lao, H.; Latieule, S.; Detellier, C. *Chem. Mater.* **1991**, *3*, 1009–1011.
(193) Nakato, T.; Kuroda, K.; Kato, C. *Chem. Mater.* **1992**, *4*, 128–132.
(194) Arhancet, J.; Davis, M. E. *Chem. Mater.* **1991**, *3*, 567–569.
(195) Fyfe, C. A.; Feng, Y.; Grondey, H.; Kokotailo, G. T.; Gies, H. *Chem. Rev.* **1991**, *91*, 1525–1543.